МИНИСТЕРСТВО ОБРАЗОВАНИЯ И НАУКИ РЕСПУБЛИКИ
КАЗАХСТАН

СӘТБАЕВ УНИВЕРСИТЕТІ

Институт металлургии и промышленной инженерии

Кафедра Инженерной физики

Имаш Әйгерім Абайқызы

The discharge kinetics and plasma chemistry study of amorphous silicon chemical vapour deposition

МАГИСТЕРСКАЯ ДИССЕРТАЦИЯ

Специальность 7М05301 Прикладная и инженерная физика

Алматы 2021

МИНИСТЕРСТВО ОБРАЗОВАНИЯ И НАУКИ РЕСПУБЛИКИ КАЗАХСТАН

СӘТБАЕВ УНИВЕРСИТЕТІ

Институт металлургии и промышленной инженерии

УДК 533.9 На правах рукописи

Имаш Әйгерім Абайқызы

МАГИСТЕРСКАЯ ДИССЕРТАЦИЯ

На соискание академической степени магистра

Название диссертации	The discharge kinetics and plasma chemistry study of amorphous silicon chemical vapour deposition
Направление подготовки	7M05301 - Прикладная и инженерная физика

Научный руководитель
К.ф.-м.н., доцент ВАК
С.К. Кунаков

"23" июня 2021г.

Рецензент
доктор PhD
Н.А.Чучвага

" 25 " июня 2021г.

ДОПУЩЕН К ЗАЩИТЕ

Нормоконтроль
Магистр естественных наук, тьютор
А.У.Толенова
"23" июня 2021г.

Заведующий кафедрой ИФ,
доктор PhD
Р.Е.Бейсенов
"23" июня 2021г .

Алматы 2021

МИНИСТЕРСТВО ОБРАЗОВАНИЯ И НАУКИ РЕСПУБЛИКИ
КАЗАХСТАН

СӘТБАЕВ УНИВЕРСИТЕТІ

Институт металлургии и промышленной инженерии

Кафедра Инженерной физики
7М05301 Прикладная и инженерная физика

УТВЕРЖДАЮ
Заведующий кафедрой
Д-р философии (PhD)
Р.Е.Бейсенов
«23» июня 2021г.

ЗАДАНИЕ
на выполнение магистерской диссертации

Магистранту *Имаш Әйгерім Абайқызы*
Тема: *The discharge kinetics and plasma chemistry study of amorphous silicon chemical vapour deposition*
Утверждена *приказом руководителя по университету № 435–М от 03"декабря 2019г.*
Срок сдачи законченной диссертации *"11"июня 2021г.*
Исходные данные к магистерской диссертации: *разработка самосогласованной математической модели для моносилановой (*SiH_4+H_2*) плазмы и оценка элементарных процессов в плазме. Получение функцию распределение энергии электронов и анализ решении уравнение Больцмана. Использование метода Монте-Карло для модели плазмохимических систем состоящей из (*SiH_4+H_2*) плазмы и электронного пучка*.
Перечень подлежащих разработке в магистерской диссертации вопросов:
а) *Анализ литературных источников по разработке модели для моносилановой (*SiH_4+H_2*) плазмы, также обзор литератур по получению тонких пленок кремния методом (PECVD).*
б) Подготовка программного кода с использованием метода Монте-Карло.
в) Решение аналитически уравнение Больцмана и получение распределение энергии электронов для моносилановой (SiH_4+H_2*) плазмы.*

Рекомендуемая основная литература:

1. Akihisa Matsuda. Microcrystalline silicon.: Growth and deviceapplication // Journal of Non-Crystalline Solids. 2004. Vol. 338. P. 112.

2. Mark J Kushner. A model for the discharge kinetics and plasma chemistry during plasma enhanced chemical vapor deposition of amorphous silicon // Journal of applied physics. 1988. Vol. 63.8. P. 2532-2551.
3. Bin Zhang and Xiaobing Zhang. Electron energy distribution functions relevant for weakly ionized SiH_4 H_2 plasma // Journal of Physics D: Applied Physics. 2020. Vol. 53.11. P. 115-201.

ГРАФИК
подготовки магистерской диссертации

Наименование разделов, перечень разрабатываемых вопросов	**Сроки представления научному руководителю**	**Примечание**
Постановка задачи	19.11.2019г. 14.01.2020г.	
Обзор литературы, выбор метода исследования	20.01.2020г. 25.08.2020г.	
Изучение и освоение метода исследования	28.01.2021г. 04.03.2021г.	
Построение моделей статистических систем и получение численного расчета	04.03.2021г. 30.04.2021г.	
Результаты исследования и их обсуждение	15.05.2021г. 10.06.2021г.	

Подписи
консультантов и нормоконтролера на законченную магистерскую диссертацию с указанием относящихся к ним разделов диссертации

Наименования разделов	**Консультанты ,И.О.Ф. (уч. степень, звание)**	**Дата подписания**	**Подпись**
Нормоконтролер	Магистра естественных наук, тьютор А.У.Толенова		

Научный руководитель: С.К. Кунаков

Задание принял к исполнению обучающийся: Ә.А.Имаш

Дата "25" июня 2021г.

ABSTRACT

Monosilane SiH_4 chemical kinetics directly depends on the electrons' energy distribution as well as from the initial electrons cloud formation by an external source of ionization. The present thesis presented electrons' energy distribution calculated from the Monte Carlo technique coupled with chemical kinetics. The proposed statistical calculations validated by correspondent Boltzmann equation solutions present a drastically different picture of chemical kinetics evolution compared with that depicted by Maxwell distribution. The electrons transport coefficients are also evaluated in strong electric fields and analyzed with the accent on the rate of useful chemical reactions directly connected with the formation of chemical vapour deposition controlled and managed by non-Maxwellian electrons energy distribution.

Also, the growth processes and the formation of hydrogenated amorphous silicon (a-Si: H) from the plasma of an H_2+SiH_4 glow discharge are considered. In the known liquid and knowledge models of plasma containing SiH_4, it is assumed that the Maxwellian distribution of the electron energy distribution function (EEDF) determines the reaction coefficients and transport coefficients in an equilibrium medium. However, EEDFs can have a bi-Maxwellian or more complex distribution, which causes large deviations in the simulation results.

This paper presents the analytical solution of the Boltzmann equation and the calculation of the EEDF for pure plasma SiH_4 and SiH_4+H_2 under stationary and non-stationary conditions. In addition, in a SiH_4+H_2 mixture, it was found that an increase in H_2 concentration increases the energy tail of electrons and the evolution of secondary electrons. Negative differential drift conductance a velocity is observed that continues to decrease with increasing H_2 and finally disappears. The electron transfer coefficients of pure SiH_4 and pure H_2 are in satisfactory agreement with the available measurements and the results of existing works.

АҢДАТПА

SiH_4 моносиланының химиялық кинетикасы электрондардың энергия арқылы таралуына, сондай-ақ сыртқы иондану көзі арқылы электрондардың бастапқы бұлтының пайда болуына тікелей байланысты. Бұл диссертациялық жұмыста химиялық кинетикамен бірге Монте-Карло әдісімен есептелген электрондардың энергия бойынша таралуы ұсынылады. Больцман теңдеуінің тиісті шешімдерімен расталған ұсынылған статистикалық есептеулер Максвеллдің таралуымен салыстырғанда химиялық кинетика эволюциясының мүлдем басқа көрінісін береді. Электронды тасымалдау коэффициенттері күшті электр өрістерінде де бағаланады және пайдалы химиялық реакциялардың жылдамдығына назар аудара отырып талданады (Максвеллианға жатпайтын электронды энергия таратуымен бақыланатын және реттелетін химиялық будың тұндыруы).

Сондай-ақ, H_2+SiH_4 қоспалы разряд плазмасынан гидрогенделген аморфты кремнийдің (a-Si: H) өсу және түзілу процестері қарастырылған. SiH_4 бар белгілі сұйық және белгілі плазмалық модельдерде электрондардың энергиялық таралу функциясының максвеллдік таралуы тепе-теңдік ортадағы реакция коэффициенттері мен тасымалдау коэффициенттерін анықтайды деп болжанады. Алайда, ЭЭТФ-на беймаксвелл немесе одан да күрделі таралуы болуы мүмкін, бұл модельдеу нәтижелерінде үлкен ауытқуларды тудырады.

Бұл жұмыста Больцман теңдеуінің аналитикалық шешімі және стационарлық және стационарлық емес жағдайларда SiH_4 және SiH_4+H_2 таза плазмасы үшін ЭЭТФ-ның есебі берілген. Сонымен қатар, SiH_4+H_2 қоспасында H_2 концентрациясының жоғарылауы электрондардың энергетикалық соңын және қайталама электрондардың шығарылуын арттыратыны анықталды. Теріс дифференциалды дрейфтің өткізгіштігі байқалады бұл – H_2 жоғарылаған сайын төмендей беретін және ақырында жоғалып кететін жылдамдық. Таза SiH4 және таза H_2 электронының тасымалдау коэффициенттері қолданыстағы өлшеулерге және қолданыстағы жұмыстардың нәтижелеріне қанағаттанарлық түрде сәйкес келеді.

АННОТАЦИЯ

Химическая кинетика моносилана SiH_4 напрямую зависит от распределения энергии электронов, а также от образования начального облака электронов внешним источником ионизации. В настоящей диссертации представлено распределение энергии электронов, рассчитанное по методу Монте-Карло в сочетании с химической кинетикой. Предлагаемые статистические расчеты, подтвержденные соответствующими решениями уравнений Больцмана, представляют совершенно иную картину эволюции химической кинетики по сравнению с той, которая изображена распределением Максвелла. Коэффициенты переноса электронов также оцениваются в сильных электрических полях и анализируются с акцентом на скорость полезных химических реакций, непосредственно связанных с образованием химического осаждения из паровой фазы, контролируемого и управляемого немаксвелловским распределением энергии электронов.

Также рассмотрены процессы роста и образования гидрированного аморфного кремния (a-Si: H) из плазмы тлеющего разряда H_2+SiH_4. В известных жидкостных и экспериментальных моделях плазмы, содержащей SiH_4, предполагается, что максвелловское распределение функции распределения энергии электронов (ФРЭЭ) определяет коэффициенты реакции и коэффициенты переноса в равновесной среде. Однако ФРЭЭ может иметь би-максвелловское или более сложное распределение, что приводит к большим отклонениям в результатах моделирования.

В данной работе представлено аналитическое решение уравнения Больцмана и расчет ФРЭЭ для чистой плазмы SiH_4 и SiH_4+H_2 в стационарных и нестационарных условиях. Кроме того, в смеси SiH_4+H_2 было обнаружено, что увеличение концентрации H_2 увеличивает энергетический хвост электронов и эволюцию вторичных электронов. Отрицательная дифференциальная дрейфовая проводимость наблюдается скорость, которая продолжает уменьшаться с увеличением H_2 и, наконец, исчезает. Коэффициенты переноса электронов чистого SiH_4 и чистого H_2 удовлетворительно согласуются с имеющимися измерениями и результатами существующих работ.

CONTENT

INTRODUCTION

Recently, installations using low-temperature plasma are being intensively introduced into the industry and everyday life. Plasma is effectively used in the field of nanotechnology, for the creation and modification of nanostructures (for example, for processing materials to increase the service life and reliability of products in mechanical engineering, create light and strong polymer composite materials, polyethylene plastics, obtain nanodispersive powders, metals, and compounds, etc.)

In modern technology, the use of micro and nanoelectronic components is very important for the production of silicon-based film materials - amorphous and polycrystalline silicon, silicon-based dielectrics, etc. Among the different methods for producing silicon films, plasma-chemical methods have some advantages. In a nonequilibrium plasma, endothermic dissociation reactions occur due to electron impact processes, which ensures the synthesis of the necessary materials at a low temperature of the working gas. The multicomponent composition, the large number of gas-phase reactions, and the high chemical activity of reagents in plasma-chemical deposition systems complicate the experimental study of such media. Therefore, in their development, mathematical modeling methods are widely used, with the help of which calculations of many parameters of gas-discharge plasma are performed, which are important from the point of view of the development and optimization of technologies [1].

The importance of monosilane to glow discharge plasma is growing rapidly; there is an urgent interest in low-pressure plasma-chemical reactors in the deposition of thin films of hydrogenated amorphous silicon, determined by the widespread use of these films as a technological material in microelectronics. Horizontal plasma-chemical reactors with two parallel electrodes are often used for plasma-assisted vapor deposition of thin films.

Plasma enhanced chemical vapor deposition (PECVD) was widely used in several technological devices [1], [2], [3] among which the first one is the most detailed primary reactions in SiH_4:H_2 plasmas are presented and described. The formation of chemical bonds and their chemical properties are also described in [4], [5] Chemical reactions usually choose the way to the equilibrium state resulting in output components and the most undesirable form [6], and [7]. To date, the simulation of gas discharges has reached a high level of perfection - complex mathematical models have been developed that contain a joint description of electromagnetic processes, electron gas kinetics, charged particle transport processes, chemical kinetics of reagents, surface processes, etc. Structurally, these models consist of several interconnected blocks (modules) that simulate individual physical and chemical processes occurring in a gas discharge [2]. Complete gas discharge models provide self-consistent ("plasma") solutions, but require significant computational resources. As an alternative to full-scale modeling, in some cases, simpler calculations are used, in which individual subsystems of the plasma medium are modeled.

Electrons due to their small masses are flexible to the impact and influence of the external electric field, which might be, applied in a number of the technical installations [8] and [9], [10]. Thus, the consideration of the processes of transport and chemical transformations of neutral particles in the discharge volume as an independent problem is of independent importance, since it allows us to estimate the spatiotemporal distribution of the plasma components responsible for the formation of films in a relatively simple way. The amount of calculations, in this case, is small. This approach has been repeatedly used to calculate the plasma composition in silane-containing gases [3-6]. Naturally, the electrical characteristics of the plasma (electron concentration, electric field strength, etc.) are introduced into the model in this case as free parameters. The values of these parameters can be taken from experimental data. In the process of modeling the chemical kinetics of plasma particles, in parallel with the solution of the main problem-the determination of the concentration of components, it is useful to consider the specific contributions of individual reactions to the increase or decrease in the most significant decomposition products. This information allows us to establish the relationship between the content of components in the gas phase and the most significant chemical reactions, as well as to investigate questions about additional channels for the formation of radicals (for example, when adding additives to the initial working mixture or complicating the description of elementary processes). Ultimately, this makes it possible to better understand both the mechanisms of the plasma chemical process and the ways of influencing it.

Chemical vapor deposition (CVD) of silicon has important technological application and solar cells are the major of them are in the following studies: [11], and [12], and [13]. Differences and similarities between μc-Si: H and a-Si: H growth reactions are analyzed in [1]. Homogeneous pyrolysis of silane [14] and detailed research up to 5 eV of SiH_4 was theoretically studded decomposition of SiH_4. The mechanism of the two following reactions was studied in [11], [15], [16]:

$$SiH_4 \rightarrow SiH_2 + H_2 \tag{1}$$

and

$$SiH_4 \rightarrow SiH_3 + H \tag{2}$$

The chemical reaction rate constants in the most detailed form are presented in [7], [17], [18]. However, the rate of chemical reactions should be corrected, especially in plasma with PECVD technologies, where the electrons are incorporated with active species tending to formation key elementary processes applied to thin films microcrystalline silicon thin films. Most of them solved by the Monte Carlo simulation technique [14], [19], [6], [20]. It was experimentally confirmed and theoretically shown that the first reaction plays the dominant role. It should be pointed out that the unimolecular decomposition of SiH_4 is accompanied by ions and excited states formation. However, the plasma phase within which the ions and excited states like SiH_4^+, H^+, H^*, H_2^*were not taken into consideration. In the author's research the electron-molecule collisions, cluster growth kinetics in dusty in low-pressure SH_4 plasma analyzed.

Hydrodynamic, hybrid, and kinetic methods for solving the Boltzmann kinetic equation and subsequent numerical models are used to study low-temperature silane plasma in this work. The time and coordinate solutions of the Boltzmann equation, which provide the velocity distributions of electrons and ions, are calculated in a kinetic manner. The Boltzmann equation is solved either directly or using statistical paths or as known by the Monte Carlo method. However, kinetic models are computationally intensive, are weakly driven by primitive assumptions, and guarantee more accurate metrics.

In addition, SiH_4 is used for Si: H film deposition .often carried out on the surfaces of the Si substrate. Therefore, any detailed study of the reactivity of the precursor must take into account the state of the surface.

1. Elementary processes in SiH4 + H2 plasma their mathematical modelling

Elemental processes include: the interaction of charged particles with each other, charged particles with uncharged particles, the interaction of uncharged particles in the system between Proceeding from this, particles of all classification, including photons, interact with a solid body (with electrodes and gas chambers). The term interaction is frequently replaced by the term collision or the term particle impact. Supposing two particles collide, both the kinetic energy of the motion of each of the particles participants in their interaction and the potential energy of each of the particles can change. According to potential energy, we mean the energy stored at the internal degrees of freedom of an atom or molecule, ie, the excitation energy of the electronic levels of an atom or molecule, the ionization energy, the excitation energy of the vibrational and rotational levels of the molecule [21, 22].

Different kinds of interactions can be separated into two groups: elastic and nonelastic interactions. By elastic collisions, changes will undergo excess nonquantum motion, that is, a steady motion of particles. Otherwise, at elastic collision only the kinetic energy of the particles and the direction of their movement changes. With a slight interaction, the changes are subject to both the kinetic and potential energy of particles [23, 24].

Let us consider the application of this law for specific examples. If in the result of the interaction of a fast electron (having mass m and speed ϑ) with atom $\mathrm{SiH_4}$ in the main state of the ionization act:

$$\mathrm{SiH_4 + e \rightarrow SiH_3 + H + e} \qquad (1.3)$$

and

$$\mathrm{H_2 + e \rightarrow H_2 + 2e} \qquad (1.4)$$

For the certainty of the above reaction, we will assume that the atom is stationary before the collision. In this example, the primary electron had sufficient kinetic energy($E = m\vartheta^2/2$) to drain the valence electron from the atom (the arrow above the electron symbol on the left side of the equation shows that the electron has a high kinetic energy). Substantially, part of the kinetic energy of the primary electron was converted into potential energy of the ionization of the atom A_i [25]. Properly speaking, part of the energy of the primary electron was also transferred in the form of the kinetic energy of ion, but, as we will see later, this is very small.

The illustration of the inner determination of the energy of the primary electron in the process of ionization of the atom from the primary state, schematically shown in the diagram of the energy content.

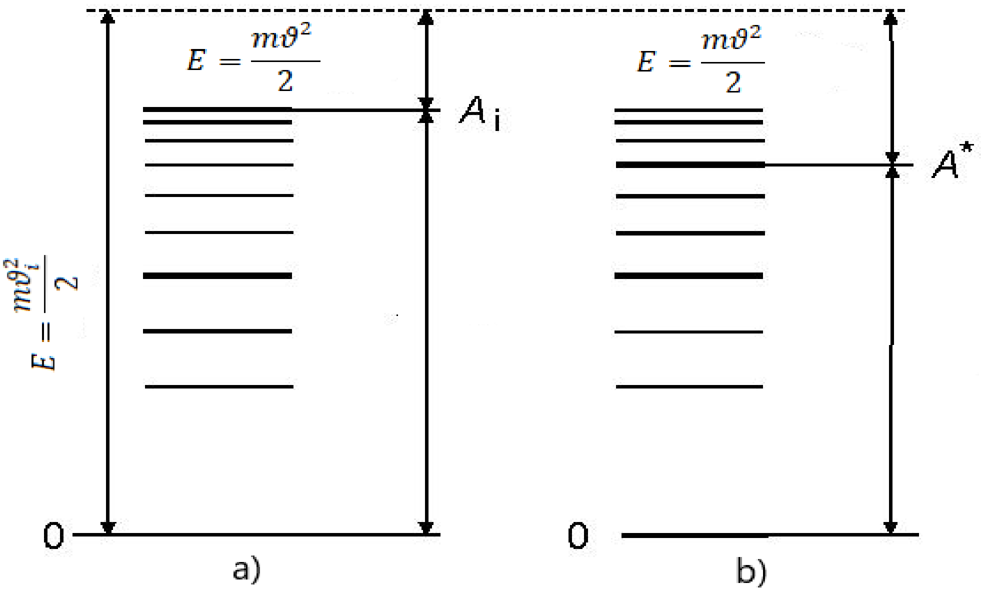

Fig. 1.1. Illustration of the law of conservation of energy in the process of ionization of an atom from the ground state (a) and excitation of an atom by an electron shock (b)

Here we can see that the total energy of the system of colliding particles before the collision was stored in the form of the kinetic energy of the electron. If we ignore the fact that after the collision, the ion took a certain velocity, it can be said that after the collision, part of the total energy preo6 was transformed into the potential ionization energy of the atom A_i, and the electrons, which are indicated in the true honor of the equation (3), redistributed the remaining energy [26].

Thus, for the destruction of the atom and the separation of the electron from it, it was necessary to expend certain energy. Therefore, in the reverse process, i.e., the formation of a neutral atom, energy must be released in some form. For the example of a collision between an ion and two electrons, the energy released during the reaction is transferred to the free electron in the form of kinetic energy [27].

From Figure 1.1 a), it can be seen that in the example considered, the free electron in the reverse process carries away the corresponding part of the energy from the system.

The reverse reaction of the ionization process is called recombination. The classification of different types of recombination and the names of different types of reactions recombination is usually associated with a channel so that it allows for the release of energy and response[28, 29]. In general, from the law of conservation of energy, it is easy to understand that at any process of particle fusion from the system, energy should be released, equal to the energy of the particles' connection.

Consider an example of an excited neutral atom A, located in the main state when connected to an electron:

$$A + \vec{e} \to A^* + e \tag{1.5}$$

In this case, part of the kinetic energy of the primary electron passes into the potential energy of the excitation of the atom A_{ex} and a small fraction of the energy is transferred to the kinetic energy of the excited particle (figure 1.1, b). In such reactions, excited atoms arise in a gas-discharge plasma, that is, atoms with a valence electron in high-energy quantum states.

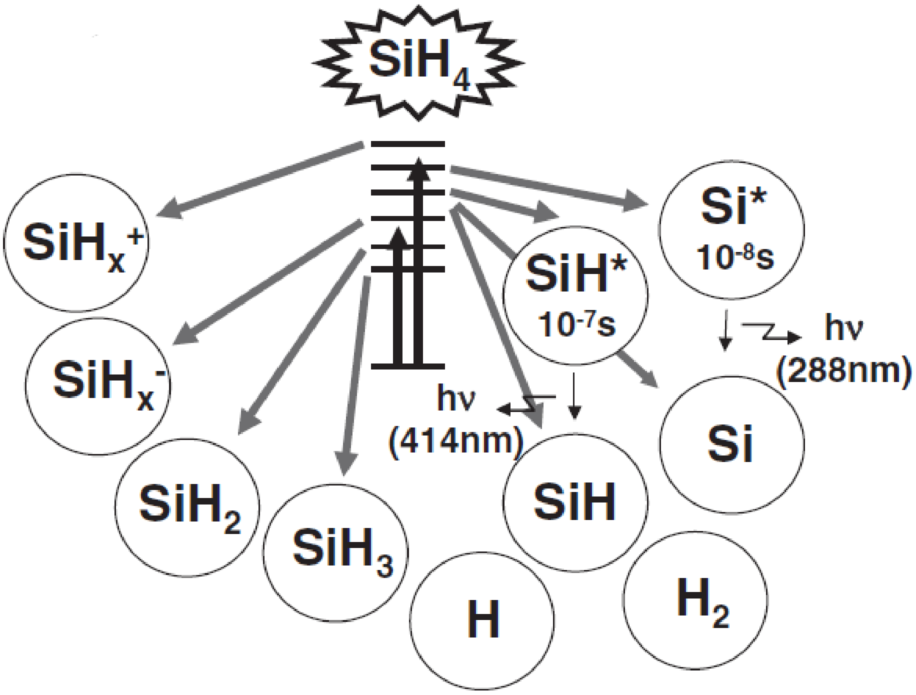

Figure – 1.2. Schematic representation of the dissociation processes for the SiH_4 molecule into various chemical compounds in plasma through their electronically excited states and hydrogen splitting.

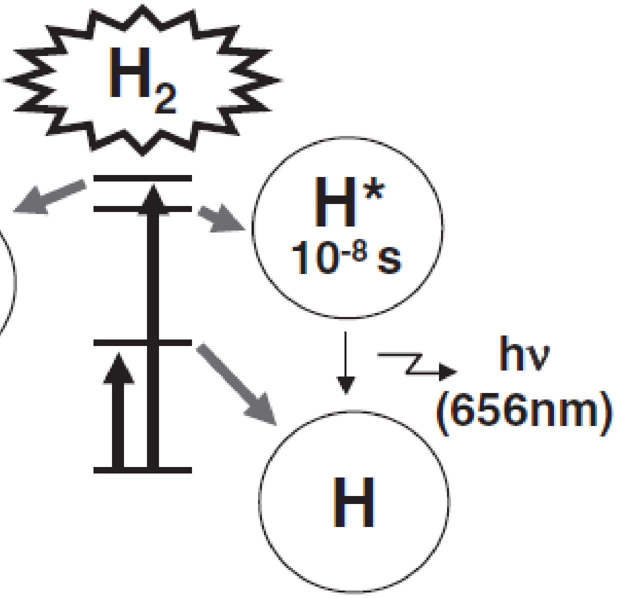

Figure – 1.3. Energy scheme electron-excited states of hydrogen H2 during the dissociation process and possible chemical compounds in the plasma.

Electronically excited states of complex molecules such as monosilane SiH4, as shown in Figure 1.1, this system is usually dissociating states, in which dissociation occurs spontaneously to SiH_3, SiH_2, SiH, Si, H_2 , and H, depending on the stereo chemical structure of the excited states of the electrons. Accordingly, spontaneous dissociation occurs without the emission of photons to return to their ground state. The hydrogen molecules also decompose into atomic hydrogen as shown in Figure 1.2. It is understood that the excitation of electrons in the ground state to a vacuum state causes an ionization process that produces new electrons and ions to maintain the plasma [26].

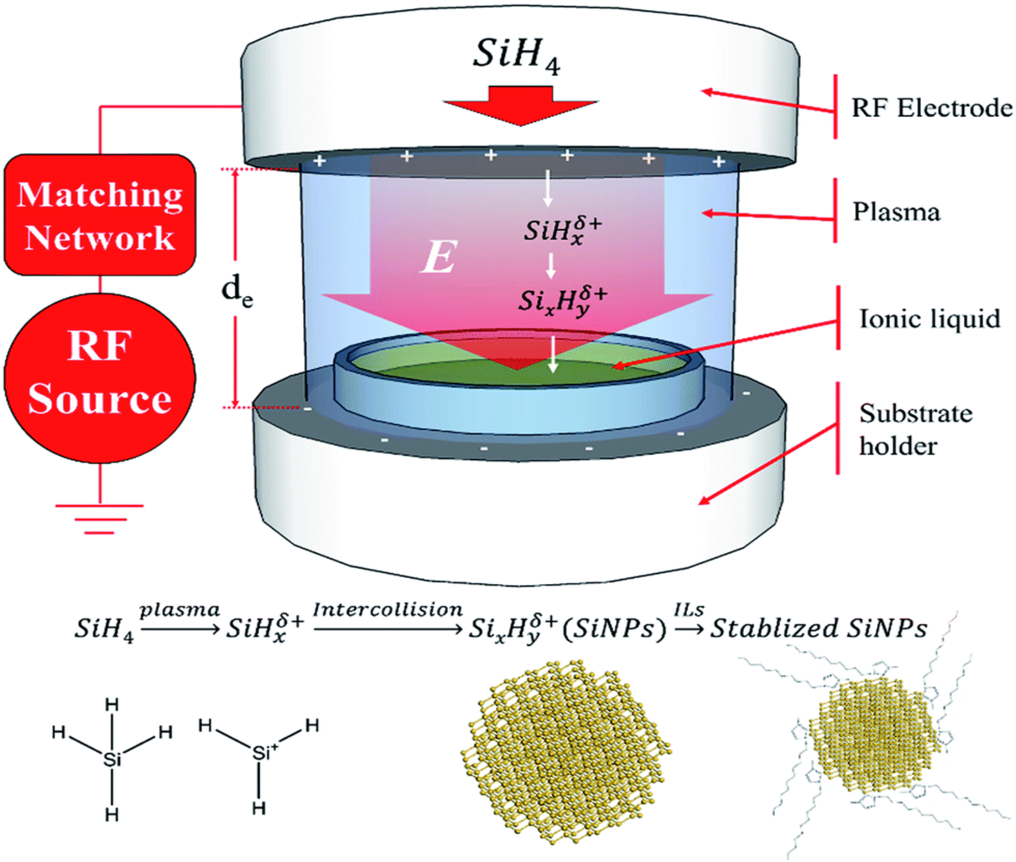

Figure 1.3. Simple scheme (PECVD) technique[5].

In this Figure 1.3, present a simple technique that takes advantage of both plasma chemical vapor deposition (PECVD) for mixtures (SiH_4+H_2) and their chemical bonds. The results that we presented and the created program can be applied to this installation.

The destruction of excited atoms can occur as a result of various reactions, including due to the reverse reaction of quenching the excited state when colliding with an electron. In this case, the potential energy of the excited atom A_{ex} is transferred to the kinetic energy of the electron. This is one of the special cases of quenching the excited state. Because of reactions of this type, an excited atom or molecule collides with another particle, because of which the excitation energy is transferred to another particle without radiation [27, 28].

Such processes are called second-order collisions or super elastic collisions.

In the present paper, the following kinetic model of elementary processes is presented:

Table 1. Elementary processes in SiH_4+H_2 plasma, irradiated by electron beam

№	Reactions	Energy(eV)	Type	Ref
R1	$\mathrm{H_2 + e \rightarrow H_2 + e}$	$3kT_e m_e/m_{(\mathrm{H_2})}$	Elastic $\mathrm{H_2}$	[19] [20]
R2	$\mathrm{SiH_4 + e \rightarrow SiH_4 + e}$	$3kT_e m_e/m_{(\mathrm{SiH_4})}$	Elastic $\mathrm{SiH_4}$	[7] [20]
R3	$\mathrm{H_2 + e \rightarrow e + 2H}$	8.9	Dissociation $\mathrm{H_2}$	[7] [19]
R4	$\mathrm{SiH_4 + e \rightarrow e + SiH_3 + H}$	5.8	Dissociation $\mathrm{SiH_3}$	[19]
R5	$\mathrm{SiH_4 + e \rightarrow SiH_2 + H_2}$	10.9	Dissociation $\mathrm{SiH_2}$	[7] [20]
R6	$\mathrm{SiH_4 + e \rightarrow SiH_2 + 2H}$	7.8	Dissociation $\mathrm{SiH_2}$	[7] [20]
R7	$\mathrm{SiH_4 + e \rightarrow e + SiH + H_2 + H}$	16.2	Dissociation SiH	[7]
R8	$\mathrm{SiH_4 + e \rightarrow SiH_3^- + H}$	6.5-11	Affinity $\mathrm{SiH_4}$	[19] [20]
R9	$\mathrm{SiH_4 + e \rightarrow e{+}SiH_4^{v13}}$	0.27	Excitation $\mathrm{SiH_4}$	[19]
R10	$\mathrm{SiH_4 + e \rightarrow e{+}SiH_4^{v24}}$	0.113	Excitation $\mathrm{SiH_4}$	[19]
R11	$\mathrm{H_2 + e \rightarrow H_2^* + e}$	11.3	Excitation $\mathrm{H_2}$	[19]
R12	$\mathrm{H_2 + e \rightarrow H_2^{j02} + e}$	0.0453	Excitation $\mathrm{H_2}$	[19] [20]
R13	$\mathrm{H_2 + e \rightarrow H_2^{j13} + e}$	0.0727	Excitation $\mathrm{H_2}$	[19] [20]
R14	$\mathrm{H_2 + e \rightarrow H_2^{v1} + e}$	0.516	Excitation $\mathrm{H_2}$	[19]
R15	$\mathrm{H_2 + e \rightarrow H_2^{v2} + e}$	1.08	Excitation $\mathrm{H_2}$	[19]
R16	$\mathrm{H_2 + e \rightarrow H_2^{v3} + e}$	1.5	Excitation $\mathrm{H_2}$	[19]
R17	$\mathrm{H_2 + e \rightarrow H_2\left(\sum Rydberg\right) + e_2}$	15.2	Excitation $\mathrm{H_2}$	[20]
R18	$\mathrm{H_2 + e \rightarrow H_2 + 2e}$	15.4	Ionization $\mathrm{H_2}$	[19] [20]
R19	$\mathrm{SiH_4 + e \rightarrow SiH_3 + H + e}$	11.9	Ionization $\mathrm{SiH_4}$	[7] [19]
R20	$H_2^+ + 2e + SiH_3^- \rightarrow H_2 + SiH_3$	≈ T e	Recombination $\mathrm{H_2}$	[20]

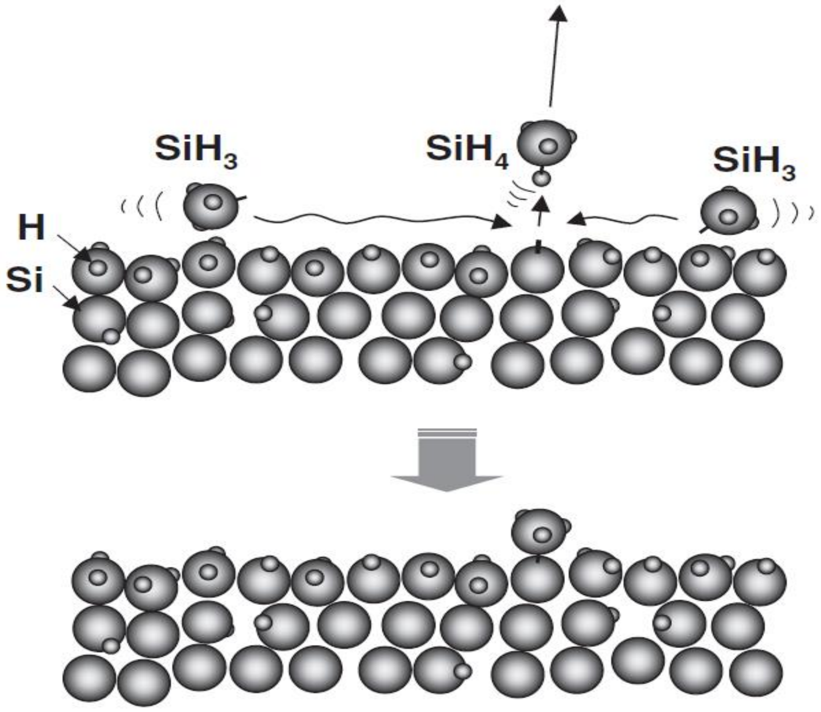

Figure – 1.4. Molecular model of a-Si:H surface growth process.

The SiH_3 radicals that reach the film growth surface begin to diffuse over the surface. During surface diffusion, SiH_3 removes the bound hydrogen covering the surface, forming SiH_4 and leaving a broken bond on the surface (formation of growth sites). Another radical, SiH_3, diffuses to the site of the broken bond on the surface and forms a Si - Si bond (film growth), as schematically shown in Figure 1.4 [29].

A common trend for all plasma-forming gases is an increase in the contribution of step-by-step (two-stage, multi-stage) processes to ionization.

Table 2. Diffusion coefficients (p = 0.1 Torr, T = 500 K) and adhesion

Component	D_k, cm^2 / s	β_k
Si	123.41	1.00
H	1149.40	0.00
H_2	677.96	0.00
SiH_4	140.30	0.00
SiH_3	150.42	0.15
SiH_2	162.10	1.00
SiH	176.18	1.00

The list of chemical reactions included in the model is shown in the table 2. The rate constants of processes involving electrons (reactions R1-R9) are determined in the model by the electron energy distribution function (EEDF) by numerically solving the one-dimensional Boltzmann equation (in the table they are marked with the symbol F). The EEDF calculation used well-known data on the cross-sections of electron collisions with H_2 and SiH_4. The values of the diffusion coefficients D_k and the adhesion coefficients β_k used in the calculation are shown in table 2 [30].

Since step processes have lower threshold energies than direct ionization, an increase in their contribution leads to a decrease in the average electron energy and electric field strength required to maintain the steady-state of the plasma. At low pressures, when the recombination of charged particles occurs mainly on the plasma-limiting walls, the effect of plasma density on electron death can only be related to a change in their effective diffusion coefficient. Naturally, the composition of the neutral component, changing the total frequency of electron collisions, will also affect their diffusion [31].

1.1.**Modelling of plasma chemical processes**

Under fixed external conditions (discharge current, pressure and composition of the initial gas mixture, gas flow rate, etc.), the field strength in a stationary plasma is set at such a level that the electronic distribution function. That depends on both the field and the composition of the gas mixture, is the atmosphere, provides the formation of such a composition of the gas phase [32, 33, 34]. Naturally, heterogeneous interactions initiated by active plasma particles can also be included in the processes that form the composition of the gas phase. The path of establishing a stationary state in the presence of chemical transformations can be divided into two branches in the first approximation [35, 36].

1) the appearance of new neutral particles in the gas phase increases the set of processes of charge generation and death, i.e. it affects the balance of electrons in geometric space.
2) the conditions for the acquisition and loss of energy by electrons (the balance in the velocity space) change, and with them the form of the electronic distribution function. Both are referred to as nonlinear effects that cause the plasma properties to depend on its density.[37,39,40]

To characterize the individual act of collision of two particles, the concept of the effective collision cross-section or the interaction cross-section σ is used. The value σ has the dimension of the area and characterizes the probability of collision of particles. The physical meaning of this value is most conveniently explained by considering the interaction of elastic balls (Figure 1.4).

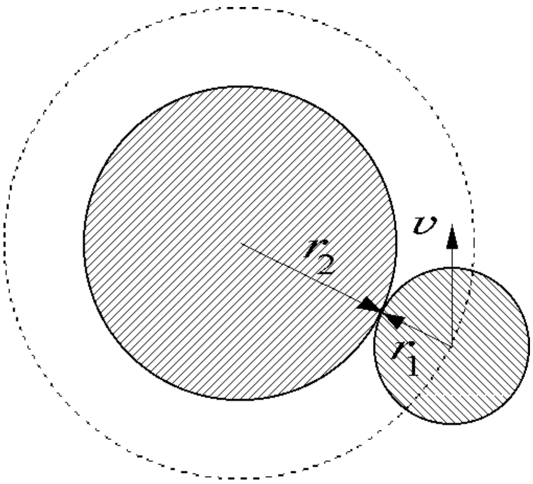

Fig. 1.5. Explanation of the concept of the cross-section for collisions of two particles.

If we consider a stationary target sphere with radius r_2, which is hit by a stream of particles with radius r_1 having a velocity v. It is clear that the number of collisions α that will occur per unit time is proportional to the density of the incoming particle flux nv, where n is the concentration of particles in the flow. Then we can write the ratio:

$$\alpha = \sigma n v \tag{1.6}$$

in which the proportionality coefficient σ will have the dimension of the area σ cm^2. This coefficient is called the interaction cross-section.

In order for the incoming sphere 1 to hit the sphere - target 2, the motion of its center must pass from the center of the target at a distance not exceeding $(r_1 + r_2)$. Obviously, for the example under consideration, the number of collisions per unit of time will be

$$\alpha = \pi(r_1 + r_2)^2 n v \tag{1.7}$$

and the collision cross-section is defined as

$$\sigma = \pi(r_1 + r_2)^2 \tag{1.8}$$

The elastic sphere model describes collisions in an ideal gas. For example, if a gas consists of particles of the same type having a diameter d, then the collision cross-section $\sigma = \pi d^2$.

It should also be noted that the process of interaction of two particles, and hence the cross-section of the interaction, is largely determined by the relative velocity of the colliding particles. In other words, the cross-section of the interaction depends on the kinetic energy of the particles involved in the reaction [41, 42, 43].

The concept of cross-section is used for a wide variety of reactions. It is useful to talk about the cross-section of the elastic interaction of an electron with an atom σ_{el} and about the dependence of this cross-section on the energy of the electron, about the ionization cross-section σ_i, about the excitation cross-section σ_{ex} of a given energy state of the atom, etc. The use of cross-sections is also convenient because this value has the property of additivity. The result of the collision of an electron with an atom can be very different. With this, a complete number of collisions for several elementary processes is equal to the number of separate processes:

$$\sigma_{tot} = \sigma_{el} + \sigma_i + \sigma_{ex} + \sigma_{diss} \ldots \tag{1.9}$$

Thus, the value of σ_{tot} characterizes the probability that a particle enters into one of the reactions that we are considering.

When considering elementary processes in a low-temperature weakly ionized plasma, many concepts of the kinetic theory of gases can be used. Consider here the meaning of the mean free path length R, i.e., the average distance that a particle travels between two collisions [44, 45].

The scattering of electrons by hydrogen and monosilane atoms in all reactions is simulated using the null collision technique [1, 2]. In this case, the experimentally known collision cross sections [6] and reaction thresholds are used. In addition, the model includes the recombination of positive and negative ions:

The reactions that we considered and calculated analytically using [18] and the results are shown in the form of a graphic.

Cross-sections for electrons and hydrogen molecules were taken from [18]. The plots corresponding to calculate with data to the cross-sections for SiH_4 and H_2 are presented in figure 1.6 and in figure 1.7, respectively.

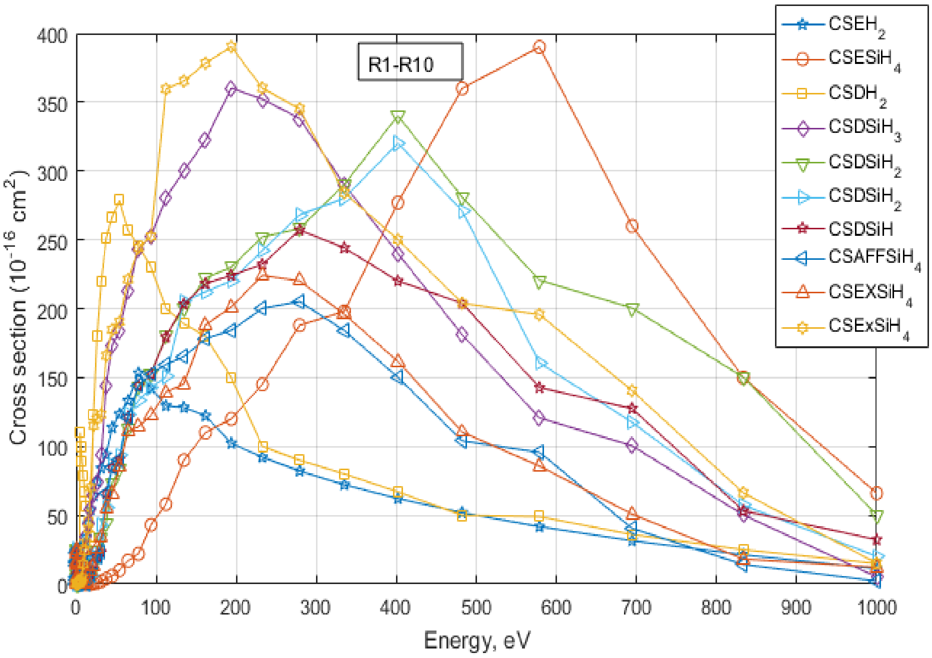

Figure 1.6: Cross sections for electron impact reactions for SiH_4 and H_2 from R1 to R10 (table 1)

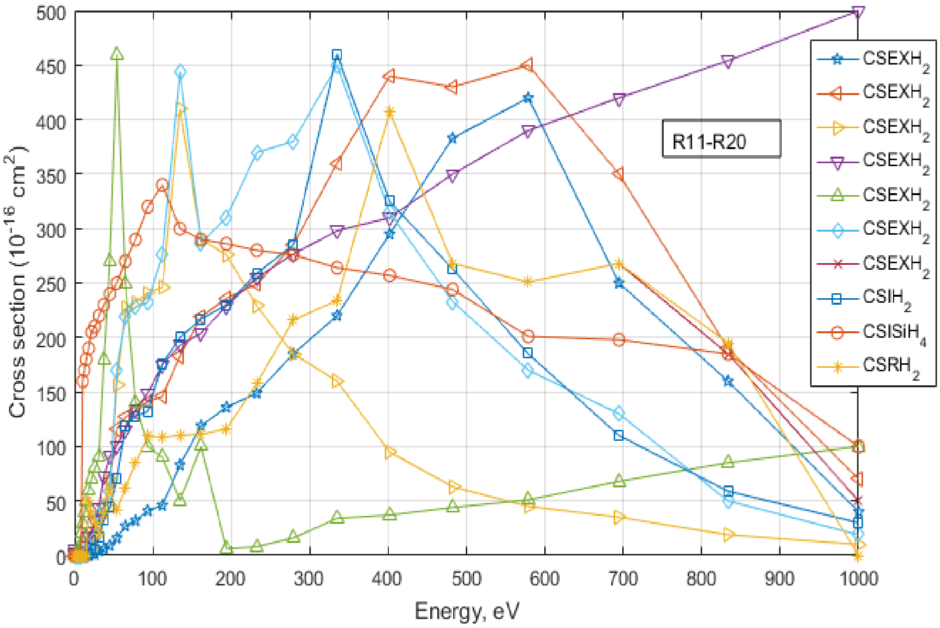

Figure 1.7: Cross sections for electron impact reactions for SiH_4 and H_2 from R11 to R20 (table 1)

Let the gas have an insignificant number of particles having an average chaotic velocity υ, which collide with the target particles, and the collision frequency is $\bar{\nu}$. It is easy to see that the average free path of the first-class particles in the main gas is determined by the ratio:

$$R = \frac{\bar{\nu}}{\upsilon} \qquad (1.10).$$

If we consider the collisions of electrons with atoms in a low-temperature weakly ionized gas discharge plasma, the relative velocity during the collision is approximately equal to the velocity of the electron, since the reduced mass of the gas particles SiH_4:H_2 is close to the mass of the electron. Hence, for the frequency of collisions, we obtain the ratio:

$$\nu_e = n_a \overrightarrow{v_e} \sigma_{ea} \qquad (1.11)$$

where $\sigma_{ea} = \pi d^2/4$ - cross-section of electron-atomic collisions in gas-kinetic theory, $\overrightarrow{v_e} = (8kT_e/\pi m)^{1/2}, T_e$ – electron temperature, m - is the mass of the electron.

Taking into account the above considerations and using the formulas (1.10) and (1.11), for the free path of an electron in a gas, we obtain the expression

$$R_e = \frac{1}{n_a \sigma_{ea}}. \qquad (1.12)$$

The concepts presented above are introduced based on the corresponding concepts for the theory describing the behavior of an ideal gas. As noted, the most significant factor in describing the processes of collisions in plasma is the dependence of the cross-sections on the energy of the particles. However, in the simplest estimates, the approximation is often used $\sigma = const$ and use the above formulas. At the same time, when we say that the cross-section of a process is large or small, we usually mean its comparison with the gas-kinetic cross-section. [46]

1.2.Kinetics of electrons in a silane $SiH_4 + H_2$ plasma

In a two-part process, two particles of plasma or a charged beam are involved in a chemical reaction. A typical example of such reactions is ionization and excitation of atoms by an electronic impact (see formulas (1.8), (1.9)).

For the description of the process of collision, the concept of the effective cross-section has been introduced. This concept is most convenient for the physics of atomic collisions, which treats individual acts of the interaction of particles. However, for the physics of a gas phase, it is often necessary to know the rate of occurrence or death of a particle of a specific sort in the plasma or the rate of reaction flow. The reaction rate refers to the number of elementary acts of birth or death of a particle per unit volume of plasma per unit time. This value is proportional to the concentrations of the particles involved in the reaction. In the future, to denote the concentration of particles, we will enclose the corresponding particle symbol in square brackets. [47]

Then, taking into account these notations, the following relations can be written for the rate of ionization of atoms by an electron impact and the rate of birth of excited particles A*:

$$\frac{d}{dt}[A^+] = K_i[e] \cdot [A] \tag{1.13}$$

$$\frac{d}{dt}[A^*] = K_{ex}[e] \cdot [A] \tag{1.14}$$

The proportionality coefficients K_i and K_{ex} included in these expressions that characterize the collision process are called reaction rate constants. The rate constant of the two-particle process has the dimension K_2 [cm^2/s].

If all the particles in the plasma had the same relative velocity during the collision, and the collision cross-section was constant, then for dimensional reasons it is easy to write: $K_2=\sigma\xi$.

However, at any given time, each particle has its speed of chaotic motion. The particle velocity distribution function $f(\xi)$ allows you to find the fraction of the total number of particles whose velocities lie in the range from ξ to $\xi+d\xi$. In addition, the cross-section of the interaction depends on the relative velocity of the colliding particles. Therefore, the reaction rate constant is introduced by averaging the product of $\sigma\xi$ over the distribution function:

$$K_2 = \langle \sigma \xi \rangle = \int_0^\infty \sigma(\xi) \xi f(\xi) d\xi \tag{1.15}$$

Since the particle velocity distribution function includes the average velocity or the average energy of the interacting particles as a parameter, the reaction constant therefore depends on the average energy of the particles or the temperature.

The collision frequency and the mean free path of the particle introduced earlier are naturally expressed in terms of the reaction constant following the formulas:

$$\nu = nK_2, R = \frac{\bar{\nu}}{nK_2} \tag{1.16}$$

where n is the concentration of target particles, $\bar{\nu}$ is the absolute average velocity of the chaotic motion of the particle, for which the average free path is calculated.

It is clear that with this entry, the difference between the relative velocity of colliding particles and the absolute velocities is taken into account when calculating the reaction constant [48].

In the triple process, three particles are involved in the collision at the same time. Usually, the triple process is a particle fusion reaction, and this process proceeds according to the following scheme:

$$A + B + C = AB + C. \tag{1.17}$$

The role of the third particle C is to carry away from the system the energy released during the formation of the AB complex. One of the examples discussed earlier is the recombination reaction (1.3), in which the electron acts as the third particle. The rate of formation of AB particles is proportional to the concentrations of the particles involved in the reaction, i.e. the differential equation for the rate of formation of AB complexes has the form:

$$\frac{d}{dt}[AB] = K_3[A] \cdot [B] \cdot [C] \tag{1.18}$$

The coefficient of proportionality has a dimension of K_3 [cm^6 / s] and is called the constant of the process.

The principle of detailed equilibrium can formulate for a system that is incomplete thermodynamic equilibrium, which following is performed.

- The total number of particles leaving the quantum state per unit time is equal to the total number of particles entering this state per unit time.
- The number of particles that leave a given state in a certain way per unit of time is equal to the number of particles that oppositely arrive in a given state [49].

Both of these statements can be disclosed. The first point says that the plasma is maintained in a stationary state, and the concentrations of particles of all types do not change over time. Whence the stationary state can be maintained in various ways. For example, the production of excited particles can occur as a result of collisions of atoms with electrons (reaction 1.5), and the death of particles can be balanced by production as a result of the spontaneous decay of excited atoms:

$$A^* \rightarrow A + h\nu \tag{1.19}$$

This situation may be typical for a plasma in a stationary state, but it is not typical for a plasma in a state of complete thermodynamic equilibrium.

Therefore, the second statement reinforces the first point. It says that for each direct reaction, there is always a reverse reaction, and in the state of thermodynamic equilibrium, the rates of the direct and reverse reactions are equal to each other.

One of the consequences of this principle is that it invites you to subtract the rate constant of the reverse reaction from the known constant of the direct reaction. For example, under conditions of thermodynamic equilibrium, for the reaction of excitation and de-excitation of an atom, we can write:

$$[A] \cdot [e]\, K_{ex} = [A^*] \cdot [e] K_q \tag{1.20}$$

whence we get

$$K_q = \frac{[A]}{[A^*]} K_{ex} \tag{1.21}$$

Maxwell’s law describes states of thermodynamic equilibrium of the temperature of all components of the plasma plane, the particle velocity distribution, and the particle distribution over the excited states is described by the Boltzmann formula. Then there is no effort for a given temperature to determine the concentrations of particles A and A*. As a result, the quenching constant of an excited atom by an electron shock is easily calculated.

2. Substructure of hydrodynamic models of gas discharges

2.1 The function of distribution of particles in plasma by speed

Consider a certain ensemble of particles whose concentration is equal to n. The particles move chaotically and change the direction of velocity when they collide with each other, as well as exchange energy. A typical example of such an ensemble of particles is a gas in a closed vessel. In general, these can be particles of any variety. To be honest, in the case of a gas-discharge plasma, it can be either atoms or gas molecules, or ions, or electrons. It is clear that at a fixed moment in time, each individual particle has its own value of absolute velocity, and the velocity itself can formally lie in the range from zero to an infinitely large value. It is true to raise the question of what is the distribution of particles in ensembles in terms of velocities [50].

In other words, if we take a certain velocity interval $\Delta\xi$ in the range from ξ to $\xi + \Delta\xi$, then the question is how to determine the size $\Delta n / n$, i.e., the fraction of particles out of their total number n, whose velocity lies in the interval $\Delta\xi$.

In general, this problem is difficult. Its solution is well known from the molecular kinetic theory of gases. In accordance with this theory, the distribution of molecules (or atoms) at speed is subject to the Maxwell law. One of the most commonly used formats for recording Maxwell's law has the form:

$$\frac{dn}{n} = 4\pi\left(\frac{M}{2\pi kT}\right)^{3/2} \xi^2 exp\left(-\frac{M\xi^2}{2kT}\right) d\xi \tag{2.1}$$

where M - is the mass of the particle, kT - is the gas temperature in energy units.

The value in the left part of the equation dn/n in the physical sense is the fraction of molecules from their total concentration n, whose velocity is in the range from ξ to $\xi + d\xi$. It can be seen that dn/n is the product of some function $f(\xi)$ by the velocity interval dv. In this case, the function $f(\xi)$ is called the Maxwell function of the velocity distribution of molecules. It has the inverse dimension of the velocity:

$$f(\xi) = 4\pi\left(\frac{M}{2\pi kT}\right)^{3/2} \xi^2 exp\left(-\frac{M\xi^2}{2kT}\right) \tag{2.2}$$

It is also possible to give an interpretation of the meaning of the particle distribution function by speed from the point of view of mathematical statistics and the theory of probability. In the terminology of the theory of the probability of a quantity, the speed of a particle in the ensemble is a certain random quantity [51, 52].

Then $f(\xi)$ - is the density of the random size distribution, and the production of $f(\xi)d\xi$ shows the confidence that the particle velocity will be in the $d\xi$ intervals. In fact, each value of the function $f(\xi)$ appears as a certain weight coefficient, showing how many particles in the ensembles can have a velocity ξ.

It is clear that if we integrate *f(ξ)* over the entire velocity range, we actually take into account all the particles, i.e. we get:

$$\int_{0}^{\infty} f(\xi)\, d\xi = 1 \tag{2.3}$$

The same result in terms of probability theory means the following: The belief that a particle has any velocity that is in the range from zero to infinity is flat units. The function of the distribution of molecules by particle speed has the form of a curve with a maximum. It is easy to show that the maximum of the curve is reached at a speed of:

$$\xi_m = \sqrt{\frac{2kT}{M}} \tag{2.4}$$

The law of molecular velocity distribution (2.1) is convenient to use by writing it in a dimensionless form, i.e. by entering a dimensionless variable ξ/ξ_m. Then, after simple transformations (2.1), we get:

$$\frac{dn}{n} = \frac{4}{\sqrt{\pi}}\left(\frac{\xi}{\xi_m}\right)^2 exp\left(-\frac{\xi^2}{\xi_m^2}\right) d\left(\frac{\xi}{\xi_m}\right) \tag{2.5}$$

The corresponding function of the distribution of molecules by speed in a size-free recording will take the form:

$$f\left(\frac{\xi}{\xi_m}\right) = \frac{4}{\sqrt{\pi}}\left(\frac{\xi}{\xi_m}\right)^2 exp\left(-\frac{\xi^2}{\xi_m^2}\right) \tag{2.6}$$

For greater clarity, the graph (figure. 2.1) is presented for the last expression.

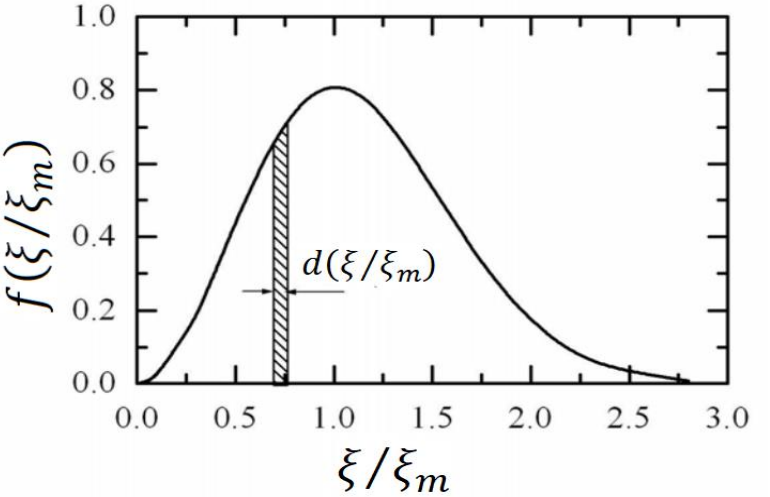

Fig. 2.1. The function of distribution Maxwell's of particles by the speed in dimensionless variables.[53]

If the temperature of the gas is known and using this graph, you can determine the fraction of particles dn/n, the velocity of which is in the $d\xi$ range. It is easy to understand that this fraction corresponds to the shaded area on the chart. It is also clear that the total area under the curve $f(\xi/\xi_m)$ is equal to one.

In the molecular kinetic theory of gases for the characterization of the ensembles, the molecules generally use the average values. For example, one of the possible standard energy characteristics is the gas temperature *kT*.

2.2 The function of particle distribution by energy

Likewise, as it is possible to operate particle distribution function by speed, we can also talk about the distribution of particles by energy. In this case, Maxwell's law gives an expression for the fraction of particles *dn / n*, the energy of which is in the interval from ε to $\varepsilon + d\varepsilon$. The expression relating the velocity and energy of a particle has the form:

$$\varepsilon = \frac{M\xi^2}{2} \tag{2.7}$$

Then, after the transformation (2.1), we obtain the following entries of Maxwell's law for the energy distribution of particles and for the energy distribution functions of particles:

$$\frac{dn}{n} = \frac{2}{\sqrt{\pi}}(kT)^{-3/2}\sqrt{\varepsilon}\, exp\left(-\frac{\varepsilon}{kT}\right) d\varepsilon \tag{2.8}$$

$$f(\varepsilon) = \frac{2}{\sqrt{\pi}}(kT)^{-3/2}\sqrt{\varepsilon}\, exp\left(-\frac{\varepsilon}{kT}\right) \tag{2.9}$$

The function of the distribution of particles by energy also has the form of a cool one with maximum, and the maximum is achieved with some energy $\varepsilon_m=kT/2$.

2.3 Formation characteristics of the electron distribution function by the speed in a gas-discharge plasma

The Maxwell function of the electron velocity distribution is often used to describe many processes in a gas-discharge plasma (at least on a qualitative level). This is quite convenient and allows you to get visual expressions when calculating the reaction constant when estimating the speed of various elementary processes when processing the results of the measured c, the entire estimate of the particle concentration and electron temperature. However, strictly speaking, this is not true.

The point is that the Maxwell distribution law is derived for an ideal gas, i.e. systems operating in thermodynamic equality and in the absence of external forces that act on particles. In this case, the transfer of energy between the particles occurs only due to the effort of communication, and the exchange of energy in each of these individuals is based on the supply of energy. This will allow entering the concept of the leading mass. For the maximum distribution of particles by speed, the anisotropic character is used, i.e. distribution of the speed of particles in all directions equally. In write the Maxwell distribution for the speed projections on the coordinates x, y, and z, then the expression for the distribution function will have the same form. In this case, the absolute speed ξ is expressed through the speed projection as follows:

$$\xi = \sqrt{\left(\xi_x^2 + \xi_y^2 + \xi_z^2\right)} \tag{2.10}$$

The situation is different for electrons in a gas-discharge plasma. As the lightest particles, electrons take energy from the electric field and give it up in ordered and inelastic collisions to heavy particles. This means that the gas is heated to account for this, that the electrons give up their kinetic energy to the atoms. At a low degree of ionization, a situation of nonequilibrium arises, when the average energy of an ensemble of an electron gas is actually higher than the average energy of an ensemble of atoms and ions [54, 55].

In addition, the distribution of the electrons at the speed of the spheres appears to be unsymmetrical, since the electrons pick up from the electric power on the ground. Then the function of the distribution by speed appears as if stretched along the field.

Finally, in addition to the acquisition of energy by the electrons from the field, there are other sources of heating of the electrons. For example, one of these sources is the production of energy by electrons in quenching collisions with excited atoms (the process is the reverse of the reaction (1.5)). In reactions of this type, fast electrons appear in the plasma, i.e., the energy distribution function is enriched with electrons with increased energy.

In general, the electron distribution function in a low-temperature plasma for specific experimental conditions must be obtained by solving the so-called chemical kinetics equation. One of the special cases for which the solution to the equation of chemical kinetics has a simple and visual form is the case of a small electric field. In a small field, electrons experience mainly elastic collisions with heavy particles, and the contribution of inelastic collisions to the formation of the particle velocity distribution function can be neglected. The electron velocity distribution at small fields can be approximated to be spherically symmetric. On the other hand, the field must still be high enough for the condition to be met:

$$eER_e \gg kT \tag{2.11}$$

where E is the electric field strength, R_e is the free path of the electron for ordered collisions.

When the latter condition is met, the problem is simplified in the sense that it is possible to read the gas atoms as stationary, i.e., the temperature of the ensemble of atoms is almost close to zero.

2.4 The ionization and excitation processes for SiH_4:H_2 plasma generated by e-beam

The process of the excitation of particles such as the atoms, molecules, or ions consists in the transition of one of the external electrons of the atom or ion, which is more energetic. If we are the main way to consider the excitation of an external one, or what the same, valence is or, in other words, optical-electronic. This terminology is used because the external electron determines the chemical properties of the atom, i.e. its valence. With a constant transition of the excited atom to a lower energy level, the quantum is usually highlighted in the optical long range. Therefore, the external electronic is also called optical.

Ionization is essentially a limiting case of excitation, when an electron bound in an atom acquires energy sufficient to detach from the atom and transition to a continuous spectrum. Due to the ionization processes, charged particles arise in the gas, and the gas is conducted, i.e., a gas discharge is ignited. In this sense, ionization is one of the main elementary processes in the discharge [56]

However, excitation also plays an extremely important role in the mechanism of plasma maintenance and current transfer. Collisions of electrons with atoms, which lead to the excitation of atoms, make up a significant part of all collisions between electrons and neutral particles. Therefore, both in the particle kinetics and in the balance of the power released in the gas, the excitation of neutral particles occupies a significant place. The presence of a large number of excited atoms and molecules changes many properties of the gas through which the current flows, for example, reduces its effective ionization potential. The result of the excitation is radiation, which affects the development of the current in the gas and is one of the external signs of the discharge and a source of information for optical diagnostics of the plasma.

Each of the elemental processes, the result of which is an excitation, can lead to ionization if there is enough energy for this. This does not mean that the same and other processes can be described in the same physical conditions. On the contrary, excitation call is a quantum process and does not fit a classic description. For ionization, many useful conclusions and a physical interpretation of the performance characteristics can be made on the basis of classical consideration. One of our goals is to show the characteristics of the phenomena of ionization and excitation in a gas-discharge plasma, without taking too much of a boost in physics. Since ionization, so and excitation are the result of the same reactions, then we would like to combine the consideration of these processes in time [57].

The classification of elementary processes to consider which causes ionization and excitement. First, it is possible to divide these processes into two groups: ionization and excitation of particles and photos. In the first group, we will separately consider collisions of particles with electrons and non-strenuous collisions of heavy particles. The electronics, in contact with the atom in the main state, can produce ionization or excitement according to the following scheme:

$$e^- + SiH_4 \rightarrow SiH_2^+ + 2H + 2e^-$$

$$e^- + H_2 \rightarrow H_2^+ + 2e^- \tag{2.12}$$

above reactions (equation 2.12) is an ionization for SiH_4, H_2

$$e^- + SiH_4 \rightarrow SiH_4^* + e^-$$
$$e^- + H_2 \rightarrow H_2^* + e^- \tag{2.13}$$

above reactions (equation 2.13) is an excitation according to the structure.

Such reactions are called reactions of direct ionization and direct excitation or ionization and excitement from the main state of the atom.

In addition, the electron can collide with an already excited atom. In this case, we are talking about the process of gradual ionization or the process of gradual excitation at a higher energy level.

3. Boltzmann equation for e-beam

The first numerical approach to the analytical solution of the Boltzmann kinetic equation was an expansion series. This approach is called the Chapman - Enskog theory [39], which writes the distribution function for equilibrium systems in the form:

$$f = f^{M} + \sum_{n=1}^{\infty} \gamma^{n} \tag{3.1}$$

where γ^{n} is a microscopic parameter, and stops the series at the first order. The first term f^{M} is the Maxwell distribution function, which gives the zero collision integral. Consequently, the transfer coefficients are associated with the perturbation f 1. This approach makes it possible to calculate transport properties with respect to specific cross sections for the reaction in plasma (SiH_4:H_2). Also, the perturbation is expanded into a polynomial series [40], allowing different degrees of approximation. The Chapman - Enskog theory is valid for microscopic deviations from the Maxwell distributions.

We should enumerate some innovative publications to adjust Boltzmann equation to study the formation of microstructural chemical plasma deposition devices and theoretical methods like in [58, 59, 60]. Following the earlier made studies [61, 62, 63, 64].

The Boltzmann equation for electron beam in the gas mixture we are presenting in the following way:

$$\partial_{e} f_{e}\left(t, \vec{r}, \overrightarrow{\xi}\right) = S_{e}^{eb} + S_{e}^{pe}(f_{e}) + S_{e}^{ion}(f_{e}) + \sum_{k} S_{e,k}^{exc}(f_{e}) + S_{e}^{el}(f_{e}) + \sum_{k} S_{e,k}^{dis}(f_{e}) + S_{e}^{rec}(f_{i} * f_{e}) \tag{3.2}$$

here $f_{e}\left(t, \vec{r}, \overrightarrow{\xi}\right)$ is distribution function of electron beam in the SiH_4:H_2 plasma by time t, radius vector $\vec{r}$ and velocity $\overrightarrow{\xi}$. It should be known that the variables t and $\vec{r}$ are hydrodynamic, but they microscopic variables and the $\overrightarrow{\xi}$ should be considered as the velocity of a particle. $S_{e}(f_{e})$ is the collisional member according to elementary processes. The collisional member in the Boltzmann equation is the result of the dynamics of pair collisions in a plasma, facilitating elastic, inelastic, and reactive processes that govern the time evolution of kinetics at the microscopic level [65]. Building a reliable database for elementary probabilities is challenging even today due to the requirements of accuracy, consistency, and completeness, issues that significantly affect the predictive power of kinetic models, not only in assessing macroscopic plasma parameters but also in shedding light on the corresponding mechanisms collisions. Modern approaches in quantum molecular dynamics are fully utilized to achieve maximum accuracy. However, a wide range of theoretical methods, including semi classical, classical, and semi-empirical, provide methods suitable for specific classes of processes, offering a favorable balance between the reliability of dynamics information and the computational burden associated with obtaining a complete dataset.

$$\int_0^{\xi_e^{max}} f_e\left(t,\vec{r},\overrightarrow{\xi}\right)d\vec{\xi} = n_e(t,\vec{r}) \tag{3.3}$$

here $n_e(t,\vec{r})$ is concentration of particles in plasma by time and radius vector.

$$\partial_e = \frac{\partial}{\partial t} + \xi_i \frac{\partial}{\partial x_i} + a_i \frac{\partial}{\partial \xi_i}. \tag{3.4}$$

Equation 5 is an auxiliary mathematical apparatus that includes the characterization of particles in a plasma.

$$f_e^p\left(t,\vec{r},\vec{\xi}\right) = \int_I^{\xi_{max}} \Omega_j^{ion}\left(\Delta E_j, \xi_j\right) f^{eb}\left(t,\vec{r},\vec{\xi}\right) d(\Delta E_j) \tag{3.5}$$

here Ω_j^{ion} is the source j-type of fragments on full differential cross-section for ionization proses, I- is ionization potential, ΔE_j is energy loss, that is equal an energy received by allocated electron and total amour of ionization potential. Further solution looks like this

$$\int_0^{\infty} \delta\left(\vec{\xi} - \overrightarrow{\xi_e^0}\right) d\vec{\xi} = 1 \tag{3.6}$$

here $\delta\left(\vec{\xi} - \overrightarrow{\xi_e^0}\right)$ is a delta function that represents at the point of the initial energy a fission fragment by the energy distribution. Based on the above data the energy of the primary electron with the law of conservation of energy for a charged electron has the form of kinetic energy as follows:

$$\varepsilon_e^{esc} = \int_0^{\xi_{max}} f_e^{pe}\left(t,\vec{r},\vec{\xi}\right) \frac{m_e \xi^2}{2} d\xi \tag{3.7}$$

here m_e is effective mass of primary electrons. The function of distribution of electron beam is following:

$$f^{eb} = n_0 \left(\frac{m_e}{E^{eb}}\right)^{\frac{3}{2}} \delta\left(\xi - \xi_0^{eb}\right) \tag{3.8}$$

then we have collisional member for ionization:

$$\begin{aligned}&S_e^{ion}\left(f_e\left(t,\vec{r},\vec{\xi}\right)\right)\\&=\sum_k\left\{n_k\int_{\xi+\sqrt{\frac{2I_k}{m_e}}}^{\xi_e^{max}}\delta\left(\xi_j'\right.\right.\\&\left.-\,G_{e,k}^{ion}\left(\xi_j',\xi_j\right)p_j^{ion}(E_e')d\xi_e'\right)\int_{I_k}^{E_0-I_k}f_j\left(\xi_j'\right)\xi_j'\,\Omega_{e,k}^{ion}(\xi_e',\Delta E_e)d(\Delta E_e)\\&\left.-\,n_k\int_0^{E_0-I_k}p_{e,k}^{ion}\left(E_j\right)f_e(\xi_e)\xi_e\Omega_{e,k}^{ion}(\xi_e',\Delta E_e)\,d(\Delta E_e)\right\}.\end{aligned}\tag{3.9}$$

Then the energy of primary electrons:

$$\varepsilon_e^{esc}=\int_0^{\xi_{max}}f_e^{pe}\left(t,\vec{r},\vec{\xi}\right)\frac{m_e\xi^2}{2}d\xi\tag{3.10}$$

Following [29] and [30] the primary electrons energy distribution equals:

$$f_e^{pe}(\varepsilon)=n_e^0\left\{\frac{m_e}{E_q}\right\}G(\varepsilon)$$

$$\begin{aligned}&G(\varepsilon)\\&=\frac{I^3}{(I+\varepsilon)^2E_q}\left\{\frac{\frac{I+\varepsilon}{I}+\frac{4}{3}\left(1-\frac{I+\varepsilon}{I}Ln\left(2.7+\left(\frac{E_q-I-\varepsilon}{I}\right)0.5\right)\right)}{1+\frac{1}{3}Ln\left(2.7+\left(\frac{E_q-I}{I}\right)0.5\right)}\right\}\end{aligned}\tag{3.11}$$

where: $\mathrm{E_q}=\dfrac{m_e(\xi_e^{eb})^2}{2}$,

here G(ε) is collision integral of primary electrons, $\mathrm{E_q}$ is kinetic energy of primary electrons with hydrodynamical variable by velocity.

Solving mathematically this Boltzmann equation with a collisional term and in a system of spatial coordinates, we found the following spectrum for primary electrons.

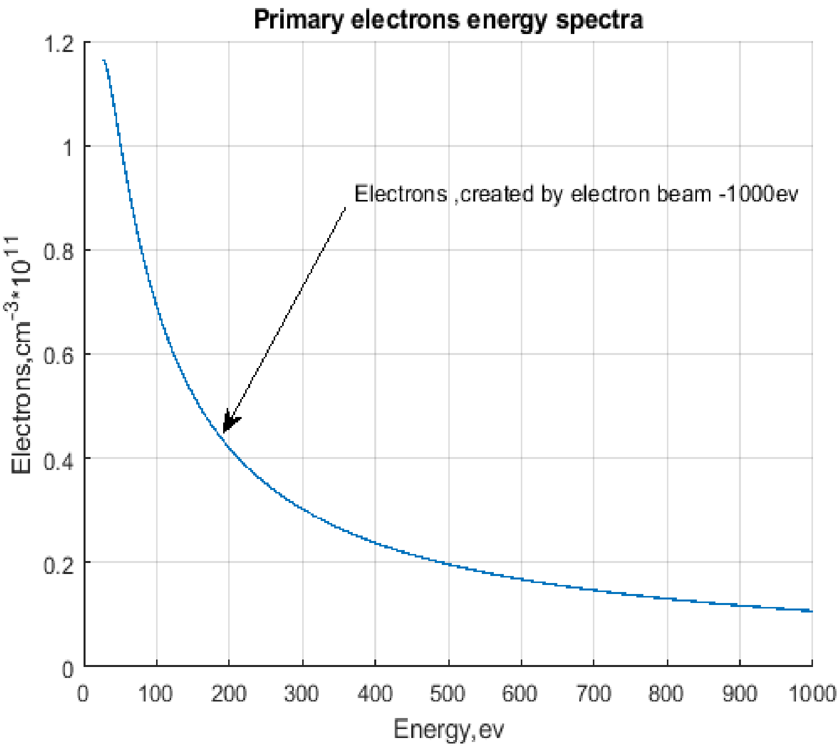

Figure 3.1. Primary electrons energy spectra by energy, calculated by the formula (3.11)

This curve (figure 3.1) can be compared [21] for reasons, the primary electron loses energy or it can be assumed that at the birth of the secondary electron this spectrum decreases, our model places the ionization peak at a slightly higher height more precisely showing the peak at high energy.

From equation, we may deduce the hydrodynamical equation for SiH_4+H_2 plasma, irradiated by electron beam:

$$\frac{\partial n_e(t,\vec{r})}{\partial t}+\nabla\vec{J_e}(t,\vec{r}) = S_e^{eb}(t,\vec{r})+S_e^{pe}(t,\vec{r})+k^T(t,\vec{r})n_e(t,\vec{r})-k^{aff}(t,\vec{r})n_e(t,\vec{r}) - k^{rec}(t,\vec{r})n_e^2(t,\vec{r}) \qquad (3.12)$$

here: $\vec{J_e}=-D_e\nabla n_e+b_e n_e\vec{E}-D_e^T\nabla T_e,\ \nabla\vec{E}=-4\pi(n_e+n^- -n^+)$

$$\frac{\partial}{\partial t}\left\{\frac{3}{2}n_e kT_e\right\}=S^{eb}E^{eb}-S^{pe}E_e^{av}-\lambda\nabla T_e-\chi(T_e-T_o) \qquad (3.13)$$

3.1 Electrons Boltzmann equation solution. Time-dependent case

We should select a three-time scale in the evolution of electrons beam energy to local Maxwellian distribution. The first one, the fast time scale lasts from zero to (figure 3.2, figure 3.3) $10^{-13}sec-10^{-9}$sec and is connected with the fast transformation of monoenergetic electrons energy of the electrons beam to the formation of primary electrons energy spectra and exciting neutrals of the testing gas. The second time scale is the slow time scale and it will be characterized by small parameter ε, which is to

$$\varepsilon = \delta\sqrt{\frac{E_{av}^{e}}{E_q}}, \qquad \delta = \frac{m_e}{M} \tag{3.14}$$

here M, m_e are mass colliding atom's. The relation between these two scales is as follows:

$$t^{slow\ scale} = \frac{t^{fast\ scale}}{\varepsilon} \tag{3.15}$$

The third time scale is slower than the second one and rings the local Maxwellian energy distribution related to the further transformation of electrons energy to heating neutrals and recombination and affinity processes. The relation of the slow elastic degradation and its corresponds to the very slow time scale last around $10^{-9} sec$ till $10^{-7,-3} sec$ and related with the first fast time scale as follows:

$$t^{maxwellization} = \frac{t^{fast\ scale}}{\varepsilon^2} \tag{3.16}$$

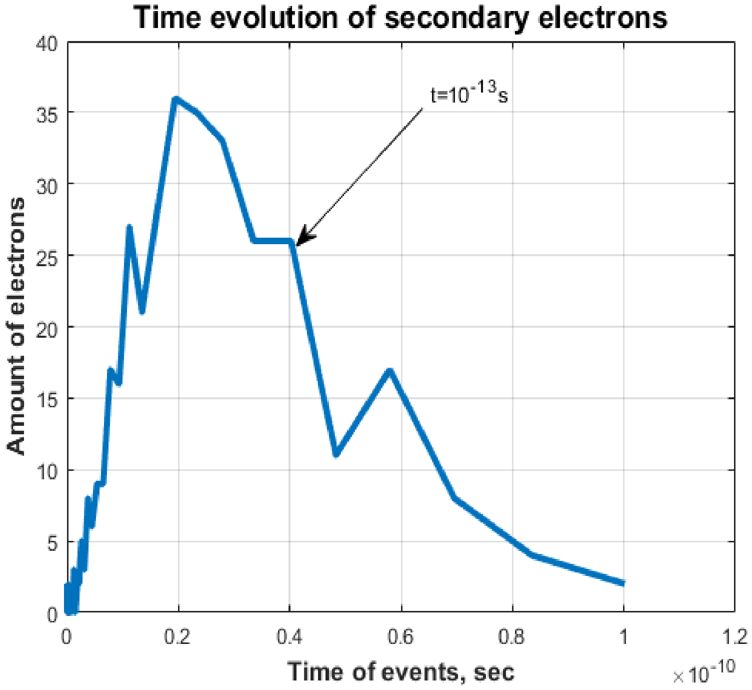

Figure 3.2. The time evolution of secondary electrons according to by formula (3.15), $t=10^{-13}$s.

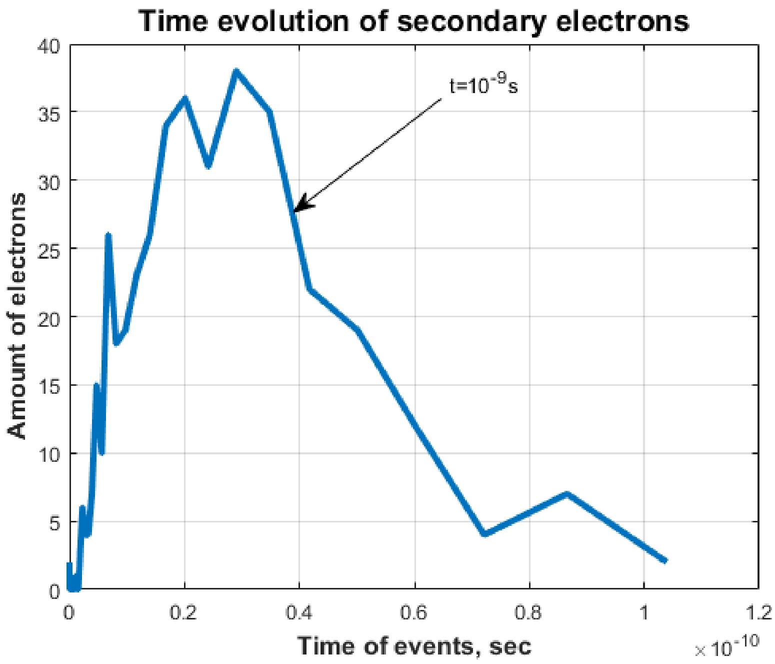

Figure 3.3. The time evolution of secondary electrons according to by formula (3.16), t=10^{-9}s.

Therefore, we may present these three types of energy distribution function as the following series:

$$\frac{\partial f_e(t,\xi)}{\partial t} = \frac{\partial f^{(0)}}{\partial t} + \varepsilon \frac{\partial f^{(1)}}{\partial t} + \varepsilon^2 \frac{\partial f^{(2)}}{\partial t} + \cdots \qquad (3.17)$$

For quick, slow, and Maxwellian time relaxation, we may present The Boltzmann equation slitting into three equation:

$$\left(\frac{\partial f}{\partial t}\right)^{(0)} = S^{eb}\big(t,\xi_0(t)\big) + n_e^{eb}\left(\frac{m_e}{E^{eb}}\right)^{\frac{3}{2}} \int_{\xi}^{\xi_0} \int_{I}^{E^{eb}} \Omega^{ion}\,(\Delta E\xi')\delta(\xi'-\xi_0)d(\Delta E)\delta\left(\xi-\Omega^{ion}(\xi',\xi)\right)\xi' d\xi' - n_e^{eb}\left(\frac{m_e}{E^{eb}}\right)^{\frac{3}{2}} \int_{I}^{E^{eb}} \Omega^{ion}\,(\Delta E,\xi)\xi f(t,\xi)d(\Delta E) \qquad (3.18)$$

Within time scale, the electrons of the electron beam are transformed into the primary electrons functions, which end the quick time scale lasting. Introducing the moderating function G(t) we get the evolution of electrons energy distribution within this time scale as follows:

$$f^{fast\ scale}(t,\xi) = n_0^e\left(\frac{m_e}{E^{eb}}\right)\delta(\xi-\xi_0) + f^{pe}(\xi) - f^{pe}(\xi)e^{-\frac{t}{\tau}} \qquad (3.19)$$

$$f^{slow\ scale}(t,\xi) = n_0^e\left(\frac{m_e}{E^{eb}}\right)\delta(\xi-\xi_0) + f^{pe}(\xi) - f^{pe}(\xi)e^{-\frac{t}{\tau}} + f^M(\xi) - f^M(\xi)e^{-\frac{t}{\varepsilon\tau_1}} \quad (3.20)$$

where: $f^M(\xi) = n_e\left(\frac{m_e}{kT_e}\right)^{\frac{3}{2}} e^{-\frac{m_e\xi^2}{kT_e}}$.

In recent years, numerical modeling has been increasingly developed with the advent of more powerful supercomputers and the development of faster and more specific algorithms. Proceeding from this, it plays an important role in this area and, along with successes in experimental work, allowed significant progress and should be achieved in the future. Dissimilar approaches to modeling have been reported in different literatures. These include analytical models, fluid models, nonequilibrium Boltzmann equations, Monte Carlo modeling and particle-in-cell models, Maxwell's equilibrium equations, non-stationary plasma-chemical environ. The combination of these models is called hybrid models.

The appearance of the phenomenon of nonequilibrium plasma is associated with the interaction of charged particles in electric fields, and in general, the kinetic description of the space charge regions is considered a clearer layout for numerical modeling. This requires asking for the conclusion of the Boltzmann equation or a Monte Carlo simulation to determine the electron distribution functions by energy and velocity. However, kinetic models strongly require a fairly large amount of time, and space charge effects are often considered within the framework of the liquid approximation.

The Boltzmann equation can be considered two additional collision processes - elastic scattering with a screened Coulomb potential and inelastic electron attachment, the cross section of which is obtained within the framework of the theory of limiting orbital motion. The investigated model of monosilane plasma includes the following ions H_2^+ SiH_2^+, SiH_3^- and excited electrons and an electron beam. The movement of these particles occurs against the background of a neutral gas, that is, a mixture of hydrogen H_2 and monosilane SiH_4. The corresponding concentration of neutral particles (monosilane and hydrogen molecules) is considered constant to maintain the plasma also in equilibrium conditions.

4. Monte Carlo method. Basic definitions

The Monte Carlo method is a statistical method for solving the transport equation for neutral particles in integral form. The main advantage of this method is that it is possible to reduce to an exact minimum the physical and geometric approximations used in solving practical problems for the development of technology. For example, the Monte Carlo method allows one to get away from the multi-group approximation, which is common for deterministic methods, and use continuous dependences of the particle behavior on energy. The disadvantage of this method is that the solution is organically difficult for the Monte Carlo method are the problems of deep passage of particles (propagating from any source through thick layers of protection) and obtaining, with good statistical accuracy, estimates of functional in very small regions of the phase volume of the system. In both cases, this is due to the low attendance of particles in the corresponding areas when using analog modeling due to the limited history sampling.

The Monte Carlo method examines the atomic structure of plasma and charged particles. The gas mixture (SiH_4:H_2) is represented by a large number of pseudo-particles, each of which represents a large number of real particles in the same position and at the same speed. At each mesh element, the number of collisions is determined according to the total cross section and a Monte Carlo approach is used to sample them. Random numbers are generated to decide which particles will collide and the result of the collision, changing the state of the particles accordingly. The convection and collision phases are repeated one after the other. With this method, the distribution function can be directly calculated with a sensitivity dependent on the number of particles.

4.1 Monte Carlo programming code description

The problematic issues of using the Monte Carlo method also include the solution of the nonstationary transport equation for monosilane SiH_4 and hydrogen H_2 molecules. Recently, due to significantly increased computing capabilities, including parallel computing, there has been significant progress here. However, the level practical calculations of various types of transient processes for large time intervals with a correct description of delayed electrons, the possibility of taking feedbacks into account, and satisfactory statistical accuracy have not yet been achieved.

The density of charged particles is six orders of magnitude less than the density of a neutral gas; therefore, only collisions of electrons with molecules of monosilane SiH_4 and hydrogen H_2 are considered. The pressure of the gas mixture (SiH_4+H_2) is about $P \approx 1 - 10^{-1}$ Torr, and the total concentration of monosilane and hydrogen is 10^{16} cm^{-3}, the concentration of electrons in the plasma is 10^{11} cm^{-3}, and the total concentration of monosilane and hydrogen ions is 10^{10} cm^{-3}. The estimated mean free path in a neutral gas for electrons is 0.01 cm, for ions, 0.001 cm. In order to break the bond between silicon and hydrogen, their bulk concentration was considered as $C(H_2) = 0.75$ for hydrogen, $C(SiH_4) = 0.25$ for monosilane. The maximum energy for a monosilane mixture is E = 1000 eV. The ratio of the mass of an electron and hydrogen is numerically calculated and is equal to $m_e/m_{H_2} = 2.7 * 10^{-4}$, for monosilane $m_e/m_{SiH_4} = 1.7 * 10^{-5}$.

A series of works were undertaken to analyze the chemical kinetics in (SiH_4+H_2), mixtures by the Monte Carlo technique. One of the electron's histories in any elementary process starts in subroutine BEGHIS. In the case when ff is not, the subject of the external field, their initial energy of the played electron equals the energy released from the e-beam source. Because of the isotropic space distribution, the directions of the secondary electron are taken randomly. It also should be noted that initial coordinates are taken within a given volume. The intensity of directly connected with neutron flux energy and spatial distribution of e-beam. Within the second loop whatever electron energy is, the integral cross section recalculated and free flight length is defined:

$$R = -\frac{ALOG(CL)}{S}, S = \sum_i N_i \sigma_{ij}\left(SiH_{4,} H_{2,} e\right) \qquad (4.1)$$

here CL-is random number with equal probability within 0,1.
The block scheme of the programming code is presented below:

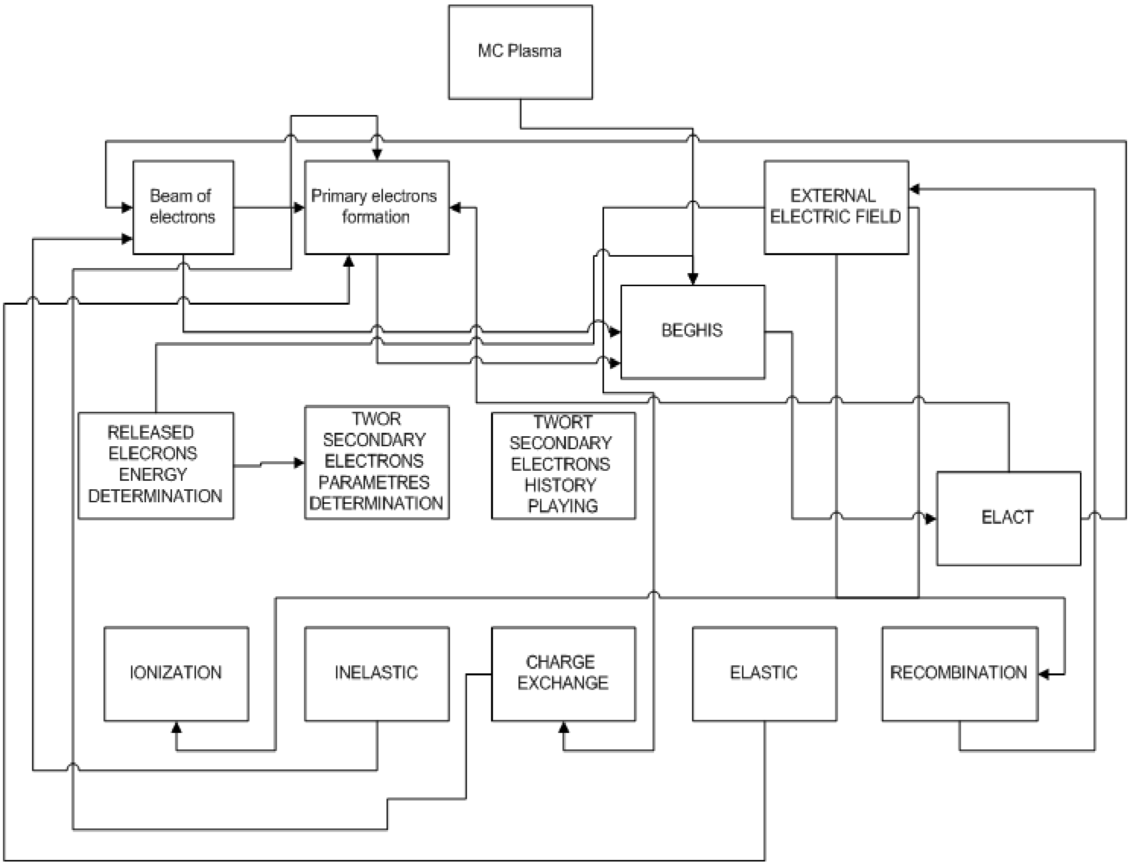

Figure 4.1. Block diagram of the calculation of the energy spectrum of the e-beam electrons by the Monte Carlo method in the (SiH_4 : H_2), excited plasma, placed in the core of a stationary electron beam.

The programming complex described in the present paper consists of three main parts: initial data input INDATA , life history trace of SiH_4+H_2 fragments and electrons degradation spectra in subroutine MKN, and recording all output data DATAOUT in less with intention txt. The main program MCN has two loops; first, one counts the number of played histories, the second loop traces the electron life history until its energy decreases to the defined minimum limit or crosses the boundaries of the given volume.

If during electron-free flight external electric field electrons do not affect charged particles (figure 4), come to target atom and calculation procedure addresses to the subroutine ELACT. In the presence of an external field, the fission fragments accelerate or lose their energy. In subroutine ELACT, one of some elementary processes choice is realized by the following rule. The normalized ladder of all possible interactions cross-sections corresponding to the current value of fission fragment energy is compiled. Then the successive comparison with random numbers brings a lucky choice for fission fragment or electron.

After the elementary process has been chosen the loss of energy, intensity, and other collision parameters are booked and returned to the main program. In the case of a three-body collision, the energy loss of the initial particle is compiled from three parts. Firstly, recoil loss, secondly, ionization potential, and thirdly the energy of the third created particle (primary electron) which has a sufficiently large range of captured energy from zero up to the total particle energy. Probability of this process inversely proportional to energy loss taken proportional to loss of energy, taken in the negative second power. The subroutines are responsible to make these calculations are in TWOW, TWOR.

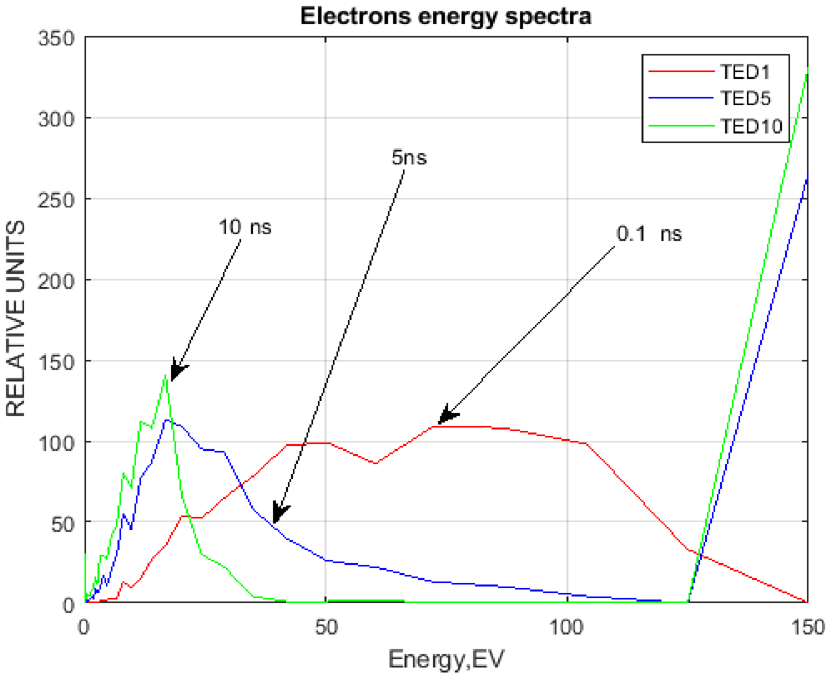

Figure 4.2. Electrons energy spectra evolution in SiH4;H2 plasma, generated by e-beam, calculated by Monte Carlo technique

Monte Carlo simulation allowed us to get the evolution the secondary electron, the mathematical solution is equations (3.19) and (3.20). Figure 4.2 shows the theoretical calculation obtained by simulation and shows that the red line corresponds to (TED9=9ns) in the ninth nanosecond time interval and shows that the electron energy has the maximum value in this interval. We considered the ten-time interval for numerical calculation and derived only (TED1=0.1ns, TED5=5ns, TED10=10ns) these intervals in graphical form. In different time intervals, the energy and number of electrons change periodically.

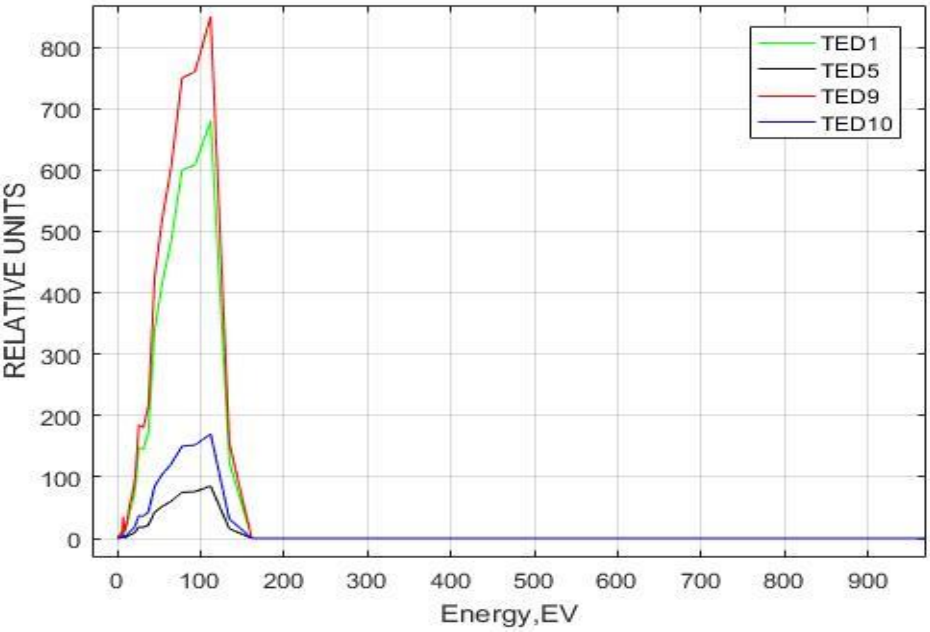

Figure 4.3 Wave-like electrons energy spectra evolution in $SiH_4 : H_2$ plasma, generated by e-beam

The acquired energy of primary electrons as well as other parameters like position coordinates, directions recorded and primary electron's histories successively played as in the fission fragments manner. The calculation code was compiled on the time depending scheme allowing and handling the processing circuits synchronized in the given time intervals and branching process for two and more generations. After each act of ionization created the primary electrons' history (independently of source-heavy fission fragments or born fast primary electron) is traced during its full life. The energy of secondary electrons created by primary ones is also randomly played and memorized in queue arrays, which then are used to trace secondary electron's histories by the LIFO rule (last in, first out). Tracking the trajectories of the primary electron's energy was carried out up to 0.1 eV. Recombination of positive particles, protons, and tritium nuclei played and tracked up the thermal region and ends counting in the thermal region until all electrons are taken from the present energy distribution of electrons histories. Integral cross-section of recombination needs the total concentration of positive ions in the plasma, which was calculated from the ionization rate, and a lifetime of the ion's history.

For monosilane, two vibrational excitation reactions are inherent, differing in the reaction threshold, and for hydrogen, three. The radicals (hydrogen atoms) formed in the reactions in a real discharge are absorbed on the walls of the chamber. Since the radicals have no charge, they are not taken into account when calculating the charge density and potential. Thus, new model particles are formed only as a result of the ionization reaction. In all reactions, except for elastic collision, the electron loses energy equal to the reaction threshold. In this work, the following types of real particles are represented as model particles: electrons and ions $SiH_4{}^+$, H^+, H_2^+, SiH_3^-. Each cell initially contains 1000 model particles of each type, a total of 21 million particles, the number of electrons in the program is 3000 per shot.

The calculation should continue until the discharge becomes stationary (until the time-averaged profile of the concentration of ions and electrons stops changing). Since the mass of the ion is much (for the SiH_2^+ ion 50,000 times) greater than the mass of the electron, then when setting the calculation time, it is necessary to focus on the ionic component of the plasma. Thus, the calculation time should significantly (several tens of times) exceed the time of flight of the ion through the interelectrode gap; with the above calculation parameters, this is more than 1000 periods or 10^{-10}s. The difficulty lies in the fact that the length of the time step must be set on the basis of the electron velocities so that the model particles-electrons do not pass more than one cell per time step (this is necessary for the stability of the calculation using the particle-in-cells method). As a result, the number of time steps in the calculation turns out to be very large (over a million). This difficulty is overcome by performing calculations on a supercomputer.

5. Chemical kinetics of radicals in hydrogen-monosilane plasma

The reaction mechanism shows a sequence of steps in the formation of chemical bonds, dangling bonds and intramolecular rearrangement, which leads to complete chemical modification. These individual stages are called elementary reactions or elementary processes. In an elementary reaction, intermediate new particles are not born; that is, none of the arrangements of atoms that arise during an elementary reaction has a lifetime longer than the duration of the molecular vibration, which usually occurs from 10^{-13} to 10^{-15} seconds.

We present the model of chemical processes in SH_4:H_2 irradiated by e-beam. We should emphasize that in the model we take into our consideration the study how the rate of formation of hydrogen excited state and ions (H^* and H^+) are influenced by e-beam and created primary electrons and generally by total electron energy distribution in the plasma. Among the sufficient number of processes, the most affected by electrons energy distribution evolving in time and space are the following ones:

$$\begin{gathered} SiH_4 + e^{eb} \rightarrow SiH_4^+ + e^{pr} + e_{\Delta E}^{eb} \\ H_2 + e^{eb} \rightarrow H_2^+ + e^{pr} + e_{\Delta E}^{eb} \end{gathered} \tag{5.1}$$

Here e^{eb} is e-beam electrons, e^{pr} - primary electrons, generated by e-beam. The next two recombination processes with thermal electrons are very sensitive to electron's energy distribution are the following:

$$\begin{gathered} SiH_4^+ + e \rightarrow SiH_4^* \\ H_2^+ + e \rightarrow H_2^* \end{gathered} \tag{5.2}$$

The active components H^+, H^* are the main participants in the formation of silicon atoms created by gradually removal and destroying away bonds with hydrogen atoms in the silanium molecule SiH_4 ended by formation of molecular hydrogen molecules:

$$\begin{gathered} SiH_4 + e \rightarrow SiH_3 + e_{\varepsilon-I} + H^* \\ H_2 + e \rightarrow H^* + H^{**} + e_{\varepsilon-I} \end{gathered} \tag{5.3}$$

Then the successive taking away the hydrogen atoms from the SiH_4 by excited H^* hydrogen atoms and hydrogen ions leads to the formation of Si:

$$\begin{gathered} SiH_4 + (H^*, H^+) \rightarrow SiH_3 + H_2^{*,+} \\ SiH_3 + (H^*, H^+) \rightarrow SiH_2 + H_2^{*,+} \\ SiH_2 + (H^*, H^+) \rightarrow SiH + H_2^{*,+} \end{gathered} \tag{5.4}$$

$$SiH + (H^{*}, H^{+}) \rightarrow Si + H_2^{*,+}$$

The law of velocity is an equation that describes how the observed reaction rate depends on the concentrations of the substances involved in the reaction. This concentration dependence can be determined experimentally. We will see that any series of elementary reactions predicts the dependence of the reaction rates on the concentrations, so one of the first checks of the proposed mechanism is that it corresponds to the speed law observed experimentally. (If the overall reaction proceeds in more than one stage and the concentration of intermediate particles becomes significant, we may need more than one equation to adequately describe the rates of all the reactions that occur.) The law of speed plays a central role in the process. our study of the reaction rate and mechanisms. We derive the velocity law from experimental measurements. We should be able to prove that the experimental velocity law is consistent with any mechanism we propose. The law of velocity, which we derive from the experimental data of velocity, is an experimental fact. Our supposed mechanism is a theory. We can stick to the idea that a theory can only be true as long as its predictions about the law of velocity agree with the experimental result. We can predict the speed laws for elementary processes with fairly simple arguments. For a mechanism involving a series of elementary processes, we can often predict the laws of velocity by making simplifying assumptions. When simplifying assumptions are inadequate, we can use numerical integration to test the agreement between the proposed mechanism and experimental observations of the dependence of the reaction rate on the concentrations of the components involved in the reaction. We will see that this experimental law of velocity can be consistent with any of several mechanisms. In such cases, we need to get additional information to distinguish between several mechanisms.

So the chemical equations in SiH_4 :H_2 are presented as follows:

$$\frac{d[SiH_4^{+}]}{dt} = S^{eb}(SiH_4) + S^{pe}(SiH_4) - \alpha_{SiH_4}^{rec}\big(f_e(t,\varepsilon)\big)[SiH_4^{+}] * n_e,$$

$$\alpha_{SiH_4}^{rec}\big(f_e(t,\varepsilon)\big) = \int_0^{\varepsilon_{max}} \sigma_{SiH_4}^{rec}(\varepsilon) f_e(t,\varepsilon) d\varepsilon,$$

$$S^{eb}(SiH_4) = \int_I^{\varepsilon_{max}} \sigma_{SiH_4}^{ion}(\varepsilon)\, f^{eb}(t,\varepsilon) d\varepsilon, \qquad (5.5)$$

$$S^{pe}(SiH_4) = \int_I^{\varepsilon_{max}} \sigma_{SiH_4}^{ion}(\varepsilon)\, f^{pe}(t,\varepsilon) d\varepsilon,$$

$$n_e(t) = \int_0^{\varepsilon_{max}} f_e(t,\varepsilon)d\varepsilon.$$

$$\frac{d[H_2^+]}{dt} = S^{eb}(H_2) + S^{pe}(H_2) - \alpha_{H_2}^{rec}\big(f_e(t,\varepsilon)\big)[H_2^+] * n_e,$$

$$\alpha_{H_2}^{rec}\big(f_e(t,\varepsilon)\big) = \int_0^{\varepsilon_{max}} \sigma_{H_2}^{rec}(\varepsilon) f_e(t,\varepsilon)d\varepsilon,$$

$$S^{eb}(H_2) = \int_I^{\varepsilon_{max}} \sigma_{H_2}^{ion}(\varepsilon)\, f^{eb}(t,\varepsilon)d\varepsilon, \tag{5.6}$$

$$S^{pe}(H_2) = \int_I^{\varepsilon_{max}} \sigma_{H_2}^{ion}(\varepsilon)\, f^{pe}(t,\varepsilon)d\varepsilon,$$

$$n_e(t) = \int_0^{\varepsilon_{max}} f_e(t,\varepsilon)d\varepsilon.$$

However, every empirical constants such as $\alpha_{SiH_4}^{rec}, \alpha_{H_2}^{rec}$ that appears in the law of speed is supposed to be called a speed constant. In a complex law, velocity constants can often be represented by more than one means. In the above example, we can split the numerator and denominator, say, to get a representation in which the constant coefficients have different values, one of which is one. Much of the remainder of this chapter is devoted to understanding the relationship between the observed overall rate of reaction and the rate of the elementary processes that contribute to it.

$$\frac{dn_e}{dt} = S^{eb} + S^{pe} - \beta_{SiH_4^+}^{rec}\, n_e[SiH_4^+] - \beta_{H_2^+}^{ion}\, n_e[H_2^+] - \beta_{SiH_4}^{aff}\, n_e[SiH_4]$$

$$-\beta_{H_2}^{aff}\, n_e[H_2],$$

here $S^{eb} = j_0^{eb} S_0$,

$$S^{pe} = \int_I^{\varepsilon_{max}} \Omega_e^{ion}(\Delta E,\varepsilon) f_e^{eb}(\varepsilon)d(\Delta E),\ f_e^{eb} = n_0^{eb}\left(\frac{m_e}{E^{eb}}\right)^{\frac{3}{2}} \delta\big(\xi - \xi_0^{eb}\big),$$

$$\beta_{SiH_4^+}^{rec}\, n_e = \int_0^\varepsilon \sigma^{rec}(\varepsilon,t) f_e(\varepsilon,t)d\varepsilon,\ \ \beta_{SiH_4^+}^{aff} n_e = \int_0^\varepsilon \sigma^{aff}(\varepsilon,t) f_e(\varepsilon,t)d\varepsilon, \tag{5.7}$$

$$\beta_{H_2^+}^{rec}\, n_e = \int_0^{\varepsilon} \sigma^{rec}(\varepsilon,t) f_e(\varepsilon,t) d\varepsilon, \quad \beta_{H_2^+}^{aff}\, n_e = \int_0^{\varepsilon} \sigma^{aff}(\varepsilon,t) f_e(\varepsilon,t) d\varepsilon.$$

$$\frac{d[H^+]}{dt} = \alpha_{H_2}^{dion}(t,\varepsilon) n_e [H_2] - \beta_{SiH_4}^{restore}[H^+][SiH_4] - \beta_{SiH_3}^{restore}[H^+][SiH_3] - \beta_{SiH_2}^{restore}[H^+][SiH_2] - \beta_{SiH}^{restore}[H^+][SiH] \qquad (5.8)$$

$$\alpha_{H_2}^{dion}(t,\varepsilon) n_e = \int_{I_d}^{\varepsilon_{max}} \sigma_{H_2}^{dion}(t,\varepsilon) f_e(t,\varepsilon) d\varepsilon$$

The main of silicon films formation is proposed to be the diffusion of SiH_3 on the boundary surface with formation SiH_4:

$$SiH_3 + SiH \rightarrow SiH_4 + Si \qquad (5.9)$$

However, the detailed mathematical models describing these diffusion processes and why the species like SiH_3 are playing the key role in these processes were not discussed. Nevertheless, we present one of the possible scenario of kinetics evolution in such a plasma taking the kinetics coefficients as functional from electrons energy distribution as a functions dependent from time and energy. The kinetics issues on the boundary surface where the crystallizations of micro-crystalline silicon μc-Si:H and amorphous silicon a-Si:H are taking place go beyond the scope of this article.

The numerical models' the vital interest to the formation of thin-film and plasma chemistry around the surface boundaries. However, for the physics of a gas phase, it is often necessary to know the rate of occurrence or death of a particle of a specific sort in the plasma or the rate of reaction flow. The reaction rate refers to the number of elementary acts of birth or death of a particle per unit volume of plasma per unit time. This value is proportional to the concentrations of the particles involved in the reaction. In the future, to denote the concentration of particles, we will enclose the corresponding particle symbol in square brackets.

$$\frac{d}{dt}[H^+] = k_{11}(t) n_e [H_2] - k_{12}[H^+][SiH_4] - k_{13}[H^+][SiH_3] - k_{14}[H^+][SiH_2] - k_{15}[H^+][SiH] \qquad (5.10)$$

$$k_{12}(t) = \int_0^{\xi_{max}} \sigma^{ion}(\varepsilon) \sqrt{\frac{2\varepsilon}{m_e}} f_e(t,\varepsilon) d\varepsilon$$

$$\frac{d}{dt}[H_1^*] = k_{21}(t) n_e [H_2] - k_{22}[H_1^*][SiH_4] - k_{23}[H_1^*][SiH_3] - k_{24}[H_1^*][SiH_2] - k_{25}[H_1^*][SiH] \qquad (5.11)$$

$$k_{21}(t) = \int_0^{\xi_{max}} \sigma_1^{exc}(\varepsilon) \sqrt{\frac{2\varepsilon}{m_e}} f_e(t, \varepsilon) d\varepsilon$$

here σ - is interaction cross-section of electron-atomic collisions in gas-kinetic theory.

$$\frac{d}{dt}[H_1^*] = k_{21} n_e [H_2] - k_{22} [H_1^*][SiH_4] \qquad (5.12)$$

$$\frac{d}{dt}[H_2^*] = k_{31} n_e [H_2] - k_{32} [H_2^*][SiH_4] \qquad (5.13)$$

The proportionality coefficients K_{1n}, K_{2n} included in these expressions that characterize the collision process are called reaction rate constants. The rate constant of the two-particle process has the dimension K [cm^2/s].

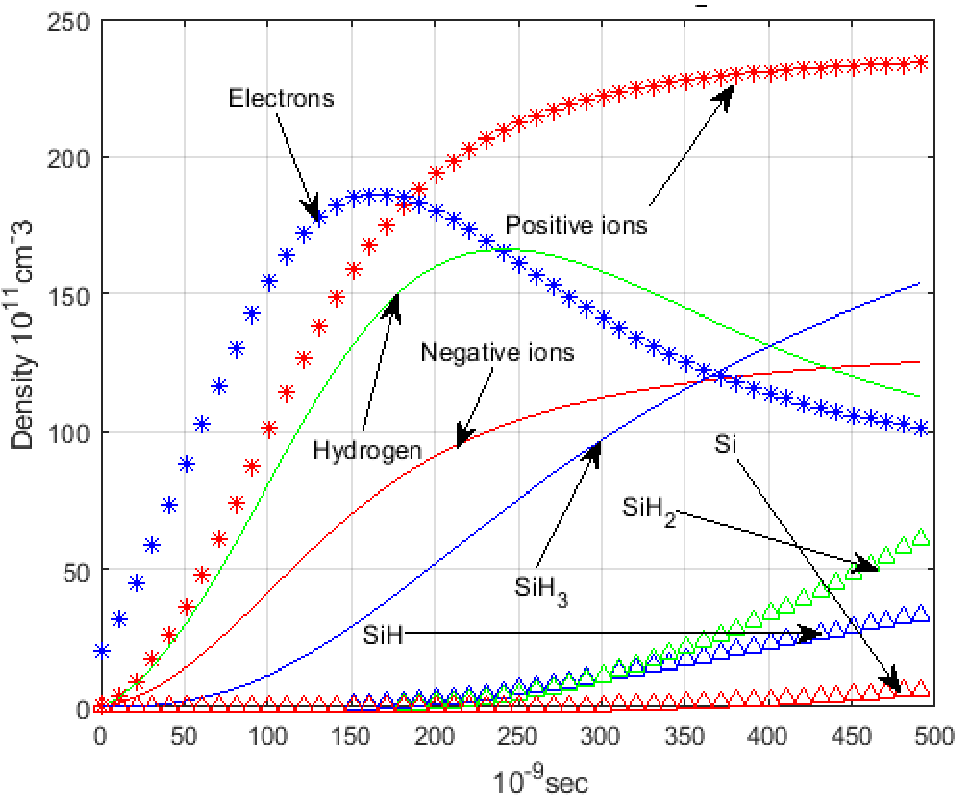

Figure 5.1. Chemical kinetics scenario in (SiH_4 : H_2), plasma, generated by e-beam

Solving the equation of chemical kinetics for plasma (SiH_4 : H_2), we were able to determine the levels of breaking bonds of silicon and hydrogen and obtained (figure 5.1) the following distribution for (SiH_4, H_2, SiH_3, SiH_2, SiH):

Our main goal is to understand the rates of chemical equilibrium in terms of competing forward and reverse reactions. In equilibrium, chemical reactions can occur rapidly; however, concentration changes are not observed since each reagent is produced by one set of reactions at the same rate as the other set. For the most part, we focus on reactions that take place in a closed system of constant volume.

In mixtures (SiH_4+H_2), the electron energy distribution function differs from the

H_2 concentration and the flow of charged electrons. Increasing the H_2 concentration not only enhances the energy tail, but also increases the negative differential conductance in the 15 Td to 80 Td range. The calculated values of the electron energy distribution function, drift velocity, and average energy in mixtures (SiH_4+H_2) are close to those in pure SiH_4 gas. The average energy in pure H_2 increases by almost several orders of magnitude. Remarkable synergy was found in the Townsend coefficient in mixtures (SiH_4+ H_2). In addition, the calculated transfer coefficients are well represented with the available experimental data.

CONCLUSION

In this work, using a diffusion model of the transfer of neutral particles, we analyzed the kinetics of reactions for the constituents (SiH_4:H_2) responsible for the formation and loss of the most important components under conditions corresponding to the deposition of amorphous silicon films in a monosilane plasma of a glow discharge.

- The time-dependent solution of Boltzmann kinetic equation solution for electrons function of energy distribution was obtained.
- Monte Carlo technique applied to the simulation of the electrons energy spectra evolution to the Maxwellian one was developed
- Relaxation of electrons energy spectra to the local Maxwellian distribution demonstrates wave-like nature
- Chemical kinetics shows drastic dependence of ions formed from the time-dependent electrons energy spectra in PECVD technology for (SiH_4 : H_2), plasma.

The time analysis of the kinetics of reactions determining the growth and loss of components can be used as a method for determining such a minimum set of reagents and reactions included in the model, which are sufficient for a quantitative description of the key plasma components at a given time interval. Reduction to a model with fewer reagents allows one to reduce computational costs while maintaining the accuracy of calculations.

REFERENCES

1. Matsuda A. Microcrystalline silicon. Growth and device application // Journal of Non-Crystalline Solids. 2004. Vol. 338. P. 112.
2. Kushner M. J. A model for the discharge kinetics and plasma chemistry during plasma enhanced chemical vapor deposition of amorphous silicon // Journal of applied physics. 1988. Vol. 63.8. P. 2532-2551.
3. Wang S. Evolution of a-Si: H to nc-Si: H transition of hydrogenated silicon films deposited by trichlorosilane using principle component analysis of optical emission spectroscopy // Materials Chemistry and Physics. 2020. Vol. 240. P. 122-186.
4. Raghunath P., andothers. Ab initio chemical kinetics for reactions of H atoms with SiH_x (x=13) radicals and related unimolecular decomposition processes // International Journal of Quantum Chemistry. 2013. Vol. 113.12. P. 1735-1746.
5. Nguyen TN, andothers. Ab Initio Chemical Kinetics for the Thermal Decomposition of SiH_4^+ Ion and Related Reverse Ion Molecule Reactions of Interest to PECVD of a-Si: H Films // Plasma Chemistry and Plasma Processing. 2017. Vol. 37.4. P. 1249-1264.
6. Phillip J. S and Kushner M.J . Monte Carlo simulation of surface kinetics during plasma enhanced chemical vapor deposition of SiO_2 using oxygen/ tetraethoxysilane chemistry // Journal of Vacuum Science & Technology A: Vacuum, Surfaces, and Films. 1993. Vol. 11.5. P. 2562-2571.
7. Babahani O, et.al. Monte Carlo simulation of chemical reactions in plasma enhanced chemical vapor deposition: From microscopic view to macroscopic results // Silicon. 2019. Vol. 11.3. P. 1267-1274.
8. Juan P. B and Ignacio M. Lattice kinetic Monte Carlo simulation of epitaxial growth of silicon thin films in H_2/SiH_4 chemical vapor deposition systems // Thin Solid Films. 2017. Vol. 634. P. 121-133.
9. Bo Da, et.al. Monte Carlo simulation study of reflection electron energy loss spectroscopy of an Fe/Si over layer sample // Surface and Interface Analysis. 2020. Vol. 52.11. P. 742-754.
10. Kimberly R. M, Alan L.M and Eduardo D.G. Storage of natural gas by adsorption on activated carbon // Chemical engineering science. 1992. Vol. 47.7. P. 1569-1579.
11. Holt. Gas Phase and Surface Kinetic Processes in Hot-Wire Chemical Vapor Deposition // MRS Online Proceedings Library Archive. 2000.
12. Alves L.L and Marques L. Fluid modelling of capacitive coupled radio-frequency discharges // a review Plasma Phys. Control. Fusion. 2012. Vol. 54. P.124012.
13. Shogo S, et.al. Silicon-Carbon alloy lm formation on Si (100) using SiH_4 and CH_4 reaction under low-energy ECR Ar plasma irradiation // Materials Science in Semiconductor Processing. 2017.

14. Kees L, et.al. Ion bombardment measurements and simulations of a low temperature VHF PECVD SiH_4 H_2 discharge in the a-Si: H to μc-Si: H transition regime // physica status solidi (a). 2016. Vol. 213.7. P. 1680-1685.
15. Timothy J.S. and Kushner M.J. Monte Carlo-fluid model of chlorine atom production in Cl_2, HCl, and CCl_2 radio-frequency discharges for plasma etching // Journal of Vacuum Science & Technology B: Microelectronics and Nanometer Structures Processing, Measurement, and Phenomena. 1992. Vol. 10.5. P. 2179-2187.
16. Marvi Z, et.al. Plasma-deposited hydrogenated amorphous silicon lms: multiscale modelling reveals key processes // RSC advances. 2017. Vol. 7.31. P. 19189-19196.
17. Tawara H, and et.al. Cross sections and related data for electron collisions with hydrogen molecules and molecular ions // Journal of Physical and Chemical Reference Data. 1990. Vol. 19.3. P. 617-636.
18. Timothy J.S., et.al. Monte Carlo-fluid hybrid model of the accumulation of dust particles at sheath edges in radio frequency discharges // Applied physics letters. 1991. Vol. 59.6. P. 638-640.
19. Sasa D, et.al. Monte Carlo analysis of ionization effects on spatiotemporal electron swarm development // The European Physical Journal D. 2014.
20. Zhang B and Zhang X. Electron energy distribution functions relevant for weakly ionized SiH_4 H_2 plasma // Journal of Physics D: Applied Physics. 2020. Vol. 53.11. P. 115-201.
21. Peck J. Modeling and Experimental process optimization for a SiH_4+ H_2 surface wave plasma discharge for silicon photovoltaics. (2014).
22. Grari M and Zoheir C. Numerical Modeling of Non-equilibrium Plasma Discharge of Hydrogenated Silicon Nitride (SiH_4/NH_3/H2). // International Journal of Engineering. 2020. Vol. 33.8. P. 1440-1449.
23. Hagelaar G.JM and Pitchford L.C. Solving the Boltzmann equation to obtain electron transport coefficients and rate coefficients for fluid models // Plasma Sources Science and Technology. 2005. Vol. 14.4. P. 722.
24. Oblapenko G, et.al. A velocity space hybridization-based Boltzmann equation solver // Journal of Computational Physics. 2020. Vol. 408. P. 109-302.
25. Othman M, Saeed R.H, et.al. Boltzmann equation studies on electron swarm parameters for oxygen plasma by using electron collision cross-sections // Zanco Journal of Pure and Applied Sciences. 2020. Vol. 32.5. P. 36-53.
26. Sydney C, Thomas G.C, and David B. The mathematical theory of non-uniform gases: an account of the kinetic theory of viscosity, thermal conduction and diffusion in gases // Cambridge university press. 1990.
27. Holstein T. Energy distribution of electrons in high frequency gas discharges // Physical Review. 1946. Vol. 70.5-6. P. 367.
28. Gryzinski M. Classical theory of atomic collisions. I. Theory of inelastic collisions // Physical Review. 1965. Vol. 138.2A. P. A336.

29. Guyot J.C, Miley G.H and Verdeyen J.T. Application of a two-region heavy charged particle model to Noble-gas plasmas induced by nuclear radiations // Nuclear Science and Engineering. 1972. Vol. 48.4. P. 373-386.
30. Lev D.T. The electron diffusion coefficient in energy in bounded collisional plasmas // IEEE transactions on plasma science. 2006. Vol. 34.3. P. 728-737.
31. Annemie B., et.al. Computer modelling of the plasma chemistry and plasma-based growth mechanisms for nanostructured materials // Journal of Physics D: Applied Physics. 2011. Vol. 44.17. P. 17-40.
32. Hunter K, et.al. DSMCSimulation of the influence of hydrogen addition on the properties of silicon deposited by HWCVD // Surface and Coatings Technology. 2019. Vol. 379. P. 125-135.
33. Sahu B.B, Han J.G, Shin K.S and Hori M. Plasma Process // Polym. 2016.
34. Li T.T, et.al. Sol. Energy Mater. Sol // Cells. 2018.
35. Stoffels E, Flikweert A.J, Stoffels W.W and Kroesen G.M.W. Plasma needle: a non-destructive atmospheric plasma source for fine surface treatment of (bio)materials // Plasma Sources Sci. Technol. 2002. Vol. 11. P. 383–8.
36. Kogelschatz U. Industrial innovations based on fundamental physics // Plasma Sources Sci. Technol. 2002 . Vol. 11. P. A1–6.
37. Bogaerts A and Gijbels R. Numerical modeling of gas discharge plasmas for various applications // Vacuum. 2003. Vol. 69. P. 37–52.
38. Hammer T. Applications of plasma technology in environmental techniques // Contrib. Plasma Phys. 1999. Vol. 39. P. 441–62
39. Hallac A, Georghiou G.E and Metaxas A.C. Three-dimensional simulation of transient gas discharge phenomena—validation // 14th Gas Discharges Conf. and their Applications (Liverpool, UK, 1–6 September). 2002. Vol. 1. P. 315–8.
40. Chapman S and Cowling T.G. The Mathematical Theory of Non-uniform Gases: An account of the kinetic theory of viscosity, thermal conduction and diffusion in gases // Cambridge: Cambridge University Press. 1970.
41. Capitelli M, Bruno D and Laricchiuta A. Fundamental Aspects of Plasma Chemical Physics // Transport (Springer Series on Atomic, Optical, and Plasma Physics. 2013. Vol. 74.
42. Esposito F, Coppola C.M and Fazio D.D. Complementarity between quantum and classical mechanics in chemical modeling. The H + HeH+ → H+ 2 + He reaction: a rigorous test for reaction dynamics methods // Phys. Chem. 2015. Vol. A 119. P. 12615–26.
43. Guo Z and Zhao T. Lattice Boltzmann model for incompressible flows through porous media // Phys. Rev. 2002. Vol. E 66. P. 036304.
44. Fan J. A generalized soft-sphere model for Monte Carlo simulation Phys // Fluids. 2002. Vol. 14. P. 4399–405.
45. Kim J. G and Boyd I. D. Monte Carlo simulation of nitrogen dissociation based on stateresolved cross sections // Phys Fluids. 2014. Vol. 26. P. 012006
46. Hagelaar G and Pitchford L. Solving the Boltzmann equation to obtain electron transport coefficients and rate coefficients for fluid models // Plasma Sources Sci. Technol. 2005. Vol. 14. P. 722.

47. Lieberman, L.A. Principles of plasma discharges and materials processing / L.A. Lieberman, A.J. Lichtenberg. - New Jersey // John Wiley & Sons. 2005. Vol. 7. P. 57.
48. Donnelly, V. M. Plasma etching: yesterday, today, and tomorrow / V.M.Donnelly, A.Kornblit // J. Vac. Sci. Technol. A. 2013. Vol. 31. P. 050825.
49. Graves, D.B. Influence of modeling and simulation on the maturation of plasma technology: feature evolution and reactor design/ D.B.Graves, M.J. Kushner // J. Vac. Sci. Technol. A. 2003. Vol .21. P. 152-156.
50. B. Tang, M. Toledano-Luque, W. D. Zhang, G. Van den Bosch, R. Degraeve, J. F. Zhang, J. van Houdt // Microelectron. Eng. 2013. Vol. 109. P. 3.
51. L. T. Mason, A. Straub, D. Inns, D. Song, A. G. Aberle // Appl. Phys. Lett. 2005. Vol. 86. P. 172108.
52. T. N. Adam, S. Bedell, A. Reznicek, D. K. Sadana, A. Venkateshan, T. Tsunoda, T. Seino, J. Nakatsuru, S. R. Shinde, J. Cryst. Growth 2010, 312, 3473.
53. A. Hikavyy, I. Zyulkov, H. Mertens, L. Witters, R. Loo, N. Horiguchi, Mat. Sci. Semicon. Proc. 2017, 70, 24.
54. M. Kondo, A. Matsuda, Thin Solid Films 2004, 457, 97.
55. J. M. Hartmann, V. Benevent, J. F. Damlencourt, T. Billon, Thin Solid Films 2012, 520, 3185.
56. Raghunath P, Nghia NT, Lin MC (2014) Ab initio chemical kinetics of key processes in the hyper golic ignition of hydrazine and nitrogen tetroxide. Adv Quantum Chem 69:253–301
57. Fernandez-Ramos A, Miller JA, Klippenstein SJ, Truhlar DG (2006) Modeling the kinetics of bimolecular reactions. Chem Rev 106:4518–4584
58. Yoshida H., Morishima Y. et al Cross sections for deexcitation of He(2 3S, 2 'S and 2 'P) by SiH4 and GeH4. // Chem. Phys. Lett. 1991. Vol. 176. P. 173-177
59. Ogawa K., Shimizu et al. Preparations of a-Si:H from Higher Silanes (SinH2n+2) with the high growth rate. // Jpn. J. Appl. Phys. 1981. Vol. 20. L639-L642
60. Hollenstein, C. Diagnostics of particle genesis and growth in RF silane plasmas by ion mass spectrometry and light scattering / C. Hollenstein, J.-L. Dorier, J.Dutta et.al. // Plasma Sour. Sci. Tech. - 1994. - Vol. 3.- P. 278-285.
61. Akdim, M. R. Modeling of dust in a silane/hydrogen plasma / M.R. Akdim, W.J.Goedheer // J. Appl. Phys. - 2003. - Vol. 94. -P. 104-109.
62. Denisenko, I. A kinetic model for an argon plasma containing dust grains / I.Denisenko, M.Y.Yu, K.Ostrikov et.al. // Phys. Plasmas. - 2004. Vol. 11. - P. 4959-4967.
63. Sukhinin, G.I. Radial distributions of dusty plasma parameters in a dc glow discharge / G.I. Sukhinin, A.V. Fedoseev // Contrib. Plasma Phys.- 2012. - Vol. 52. - P. 756-760.
64. Цендин, Л.Д. Нелокальная кинетика электронов в газоразрядной плазме / Л.Д. Цендин // Успехи физ. наук. - 2010. - Т.180. - С. 139-164.
65. BOLSIG+: Electron Boltzmann equation solver / G.J.M. Hagelaar. - Toulouse: Universite Paul Sabatier. - 2018. http://www.bolsig.laplace.univ-tlse.fr